Supplementary Information (ESI)

(BB)-Carboryne Complex of Ruthenium: Synthesis by Double B–H Activation at a Single Metal Center

Bennett J. Eleazer[a], Mark D. Smith[a], Alexey A. Popov[b]*, and Dmitry V. Peryshkov[a]*.

a). Department of Chemistry and Biochemistry, University of South Carolina, 631 Sumter St., Columbia, South Carolina 29208, United States.
b). Leibniz Institute for Solid State and Materials Research, Helmholtzstrasse 20, 01069 Dresden, Germany.

Experimental

All synthetic manipulations were carried out either in a nitrogen-filled drybox or on an air-free dual-manifold Schlenk line, unless stated otherwise. Compounds **2**, **3**, **4**, **5**, and **6** were found to be moderately stable on air in a solid state. The solvents were sparged with nitrogen, passed through activated alumina, and stored over activated 4 Å Linde-type molecular sieves. Benzene-d^6 was degassed and stored over activated 4 Å Linde-type molecular sieves. NMR spectra were recorded using Varian spectrometers at 400 (^{1}H), 100 (^{13}C), 162 (^{31}P), 128 (^{11}B) MHz, reported in δ (parts per million) and referenced to the residual ^{1}H/^{13}C signals of the deuterated solvent or an external 85% H_3PO_4 (^{31}P (δ): 0.0 ppm) and $BF_3(Et_2O)$ (^{11}B(δ): 0.0 ppm) standards. J values are given in Hz. Midwest Microlab, Indianapolis, Indiana provided the elemental analysis results.

POBOP-H ligand precursor (POBOP = 1,7-OP(*i*-Pr)$_2$-*m*-carboranyl) was prepared using the previously reported procedure.[1] $[Ru(CO)_3Cl_2]_2$ (Strem), *m*-carborane $C_2B_{10}H_{12}$ (Katchem), ethyl propiolate, 3-hexyne, $BH_3(SMe_2)$ in THF, and iodine were used as received.

Synthesis of (POBBOP)Ru(CO)$_2$ BB-carboryne complex (POBBOP = 1,7-OP(*i*-Pr)$_2$-2,6-dehydro-*m*-carborane) (2)

A portion of $[Ru(CO)_3Cl_2]_2$ (0.125 g; 0.244 mmol) was added to a solution of (POBOP)H (0.200 g; 0.49 mmol, 1.02 equiv.) in benzene (2 mL). The solution was stirred at room temperature for 2 h until gas evolution ceased. The reaction mixture was transferred to a J. Young valve NMR tube and heated at 90 ºC for 8 h. An excess of NEt_3 (0.350 g; 3.46 mmol, 7.0 equiv.) was added and the reaction mixture was heated at 90 ºC for 16 h. The resulting suspension was dried under vacuum, triturated with toluene, and filtered. The filtrate was evaporated and recrystallized from a mixture of toluene and hexanes at –30 ºC producing a colorless crystalline product. Yield: 0.251 g, 0.222 mmol, 91%.

^{1}H NMR (C_6D_6): δ 4.5–1.5 (br m, 8H, B*H*), 1.80 (m, 4H, P(C*H*(CH$_3$)$_2$), 1.00 (m, 24H, P(CH(C*H*$_3$)$_2$). **^{11}B{^{1}H} (C_6D_6)**: δ –2.8 (*B*-Ru), –10.8 (*B*-H), –12.9 (*B*-H), –16.7 (*B*-H). **^{13}C (C_6D_6)**: δ 202.8 (Ru-*C*O), 115.3 (*C*$_2$B$_{10}$H$_8$), 30.7 (P(*C*H(CH$_3$)$_2$), 16.8 (P(CH(*C*H$_3$)$_2$). **^{31}P{^{1}H} (C_6D_6)**: δ 217.6. Selected bands in the IR spectrum, cm^{-1}: 2990–2880 (br, CH), 2600 (br, BH), 2010 (strong, Ru-CO), 1958 (strong, Ru-CO). Found: C, 34.10; H, 6.49. Calcd. for $C_{16}H_{36}B_{10}O_4P_2Ru$: C, 33.99; H, 6.42.

Synthesis of (POBOP)Ru(Cl)(CO)$_2$ complex (3)

An excess of aqueous HCl (0.05 mL, 3M) was added to a solution of (POBBOP)Ru(CO)$_2$ (**2**) (0.020 mg; 0.035 mmol) in C_6D_6 (1 mL). The reaction mixture was stirred at room temperature for 4 h. The resulting pale yellow solution was dried under vacuum, triturated with hexanes, and filtered. The filtrate was evaporated and recrystallized from hexanes at –30 ºC producing a colorless crystalline product. Yield: 0.020 g, 0.032 mmol, 92%.

^{1}H NMR (C_6D_6): δ 4.00–1.50 (br, 9H, $C_2B_{10}\mathit{H}_9$), 2.92 (m, 2H, $P(C\mathit{H}(CH_3)_2)$, 2.54 (m, 2H, $P(C\mathit{H}(CH_3)_2)$ 1.25 (dd, 6H, $P(CH(C\mathit{H}_3)_2))$, 1.09 (dd, 6H, $P(CH(C\mathit{H}_3)_2))$, 0.84 (dd, 12H, $P(CH(C\mathit{H}_3)_2))$. **^{11}B{^{1}H} (C_6D_6)**: δ 7.4 (s, *B*Ru), –9.4 (*B*H), –11.4 (*B*H), –12.2 (*B*H), –13.8 (*B*H), –14.5 (*B*H), –17.6 (*B*H). **^{13}C (C_6D_6)**: δ 197.7 (Ru-*C*O), 196.4 (Ru-*C*O), 104.6 (C_2B_{10}), 35.2 ($P(\mathit{C}H(CH_3)_2)$, 28.5 ($P(\mathit{C}H(CH_3)_2)$, 17.6 ($P(CH(\mathit{C}H_3)_2)$, 15.5 ($P(CH(\mathit{C}H_3)_2)$. **^{31}P{^{1}H} (C_6D_6)**: δ 214.9. Selected bands in the IR spectrum, cm^{-1}: 2970–2880 (br, CH), 2610 (br, BH), 2034 (strong, Ru-CO), 1980 (strong, Ru-CO). Found: C, 32.04; H, 6.35. Calcd. for $C_{16}H_{37}B_{10}ClO_4P_2Ru$: C, 31.93; H, 6.19.

Synthesis of (POBOP)Ru(CO)$_2$(C≡CCO$_2$Et) complex (4)

A portion of ethyl propiolate (0.050 g; 0.51 mmol, 9.5 equiv.) was added to a solution of (POBBOP)Ru(CO)$_2$ (0.030 g; 0.053 mmol) in C_6D_6 (1 mL). The reaction mixture was heated at 75 ºC for 6 h. The resulting yellow solution was dried under vacuum, and washed with 3×5 mL of hexanes to yield an orange solid. Yield: 0.034 g, 0.050 mmol, 94%.

^{1}H NMR (C_6D_6): δ 4.50–1.00 (br, 9H, $C_2B_{10}\mathit{H}_9$), 3.69 (q, 2H, $CO_2C\mathit{H}_2CH_3$), 2.72 (m, 2H, $P(C\mathit{H}(CH_3)_2)$, 2.24 (m, 2H, $P(C\mathit{H}(CH_3)_2)$, 1.22 (dd, 6H, $P(CH(C\mathit{H}_3)_2))$, 0.98 (dd, 6H, $P(CH(C\mathit{H}_3)_2))$, 0.62 (overlapping 12H, $P(CH(C\mathit{H}_3)_2)$ and 3H, $CO_2CH_2C\mathit{H}_3$). **^{11}B{^{1}H} (C_6D_6)**: δ 6.0 (*B*Ru), –7.5 to –18.8 (*B*H). **^{13}C (C_6D_6)**: δ 197.2 (Ru-*C*O), 153.1 (*C*≡*C*CO$_2$Et), 114.9 (C_2B_{10}), 107.14 (*C*≡*C*CO$_2$Et), 104.3 (*C*≡*C*CO$_2$Et), 59.9 ($C{\equiv}CCO_2\mathit{C}H_2CH_3$), 36.9 ($P(\mathit{C}H(CH_3)_2)$, 29.6 ($P(\mathit{C}H(CH_3)_2)$, 18.1 ($C{\equiv}CCO_2CH_2\mathit{C}H_3$), 15.9 ($P(CH(\mathit{C}H_3)_2)$, 15.3 ($P(CH(\mathit{C}H_3)_2)$, 13.8 ($P(CH(\mathit{C}H_3)_2)$. **^{31}P{^{1}H} ($C_6D_6$)**: δ 218.3. Selected bands in the IR spectrum, cm^{-1}: 2970–2880 (br, CH), 2600 (br, BH), 2109 (C≡C), 2036 (strong, Ru-CO), 1994 (strong, Ru-CO). Found: C, 38.36; H, 6.53. Calcd. for $C_{21}H_{42}B_{10}O_6P_2Ru$: C, 38.01; H, 6.38.

Synthesis of (POB(I)OP)Ru(I)(CO) complex (5)

A portion of I_2 ((0.008 g; 0.03 mmol, 1.1 equiv.) was added to a solution of (POBBOP)Ru(CO)$_2$ (0.015 g; 0.03 mmol) in C_6D_6 (1 mL). The reaction mixture was kept at 22 ºC for 30 min. The resulting yellow solution was dried under vacuum, and triturated with ether. The ether extract was evaporated producing a yellow crystalline product. Yield: 0.021 g, 0.026 mmol, 86%.

^{1}H NMR (C_6D_6): 4.00–1.00 (br, 9H, $C_2B_{10}\mathit{H}_9$), 3.03 (m, 2H, $P(C\mathit{H}(CH_3)_2)$, 2.68 (m, 2H, $P(C\mathit{H}(CH_3)_2)$ 1.39 (dd, 6H, $P(CH(C\mathit{H}_3)_2))$, 1.31 (dd, 6H, $P(CH(C\mathit{H}_3)_2))$, 1.21 (dd, 6H, $P(CH(C\mathit{H}_3)_2))$, 0.93 (dd, 6H, $P(CH(C\mathit{H}_3)_2))$. **^{11}B{^{1}H} (C_6D_6)**: δ 1.3 (*B*Ru), -10.3 (*B*H), -12.8 (*B*H), -15.0 (*B*H and *B*I), -20.0 (*B*H). **^{13}C (C_6D_6)**: δ 206.1 (Ru-*C*O), 102.9 (C_2B_{10}), 35.4 ($P(\mathit{C}H(CH_3)_2)$, 20.5($P(\mathit{C}H(CH_3)_2)$, 16.4 ($P(CH(\mathit{C}H_3)_2)$. **^{31}P{^{1}H} (C_6D_6)**: δ 200.4. Selected bands in the IR spectrum, cm^{-1}: 2960–2860 (br, CH), 2600 (br, BH), 1963 (strong, Ru-CO). Found: C, 23.11; H, 4.72. Calcd. for $C_{15}H_{36}B_{10}I_2O_3P_2Ru$: C, 22.77; H, 4.59.

Synthesis of (POBOP)(EtC=CEt)Ru(CO)$_2$ complex (6).

An excess of 3-hexyne (0.25 mL) was added to a solution of (POBBOP)Ru(CO)$_2$ (0.020 g; 0.035 mmol) in $\mathrm{C_6D_6}$ (1 mL). The reaction mixture was irradiated with a mercury vapor 200 WPI UV lamp (American Ultraviolet UV010) for 1 hour. The resulting brown solution was dried under vacuum, triturated with acetonitrile (3×3 ml), and filtered to yield a white solid. Yield: 18 mg, 0.031 mmol, 88%.

^{1}H NMR ($\mathrm{C_6D_6}$): δ 4.00–1.00 (br, 9H, $\mathrm{C_2B_{10}}H_9$), 2.68 – 2.61 (overlapping m, 2H, $\mathrm{P(C}H\mathrm{(CH_3)_2}$ and q, 4H, $\mathrm{(C)C}H_2\mathrm{CH_3}$), 2.49 (m, 2H, $\mathrm{P(C}H\mathrm{(CH_3)_2)}$, 1.21 (t, 3H, $\mathrm{(C)C}H_2\mathrm{CH_3}$), 1.11–1.03 (overlapping t, 3H, $\mathrm{(C)C}H_2\mathrm{CH_3}$ and dd, 24H, $\mathrm{P(CH(C}H_3\mathrm{)_2)}$. **^{11}B{^{1}H}** ($\mathrm{C_6D_6}$): δ 8.0 (*B*Ru), 0.7 (*B*C), -13.0 (*B*H), -14.3 (*B*H), -16.1 (*B*H), -20.8 (*B*H). **^{13}C** ($\mathrm{C_6D_6}$): δ 198.8 (Ru-*C*O), 178.3 ($C\mathrm{CH_2CH_3}$), 104.3 ($C_2\mathrm{B_{10}}$), 37.8 ($\mathrm{P(}C\mathrm{H(CH_3)_2)}$, 32.3 ($\mathrm{P(}C\mathrm{H(CH_3)_2)}$, 18.1 ($\mathrm{P(CH(}C\mathrm{H_3)_2)}$, 17.7 ($\mathrm{P(CH(}C\mathrm{H_3)_2)}$, 16.4 ($\mathrm{C}C\mathrm{H_2CH_3}$), 16.3 ($\mathrm{P(CH(}C\mathrm{H_3)_2)}$, 1.05 ($\mathrm{CCH_2}C\mathrm{H_3}$). **^{31}P{^{1}H}** ($\mathrm{C_6D_6}$): δ 213.2. Selected bands in the IR spectrum, cm^{-1}: 2970–2870 (br, CH), 2600 (br, BH), 2008 (strong, Ru-CO), 1968 (strong, Ru-CO). Found: C, 40.57; H, 7.18. Calcd. for $\mathrm{C_{22}H_{46}B_{10}O_4P_2Ru}$: C, 40.80; H, 7.16.

Synthesis of POB(BH$_3$)OP)Ru(CO)$_2$ complex (7).

An excess of a solution of $\mathrm{BH_3(SMe_2)}$ in THF (0.25 mL, 3M solution in THF, 0.75 mmol) was added to a solution of (POBBOP)Ru(CO)$_2$ (0.020 g; 0.035 mmol) in $\mathrm{C_6D_6}$ (1 mL). The reaction mixture was heated at 90 ºC for 12 h in a J. Young valve NMR tube. The resulting pale yellow solution was dried under vacuum, triturated with acetonitrile (3×5 ml), and filtered to yield a white solid. Yield: 20 mg, 0.033 mmol, 95%.

^{1}H NMR ($\mathrm{C_6D_6}$): δ 4.00–1.00 (br, 9H, $\mathrm{C_2B_{10}}H_9$), 2.50 (overlapping m, 4H, $\mathrm{P(C}H\mathrm{(CH_3)_2)}$, 1.08 (dd, 12H, $\mathrm{P(CH(C}H_3\mathrm{)_2))}$, 0.88 (dd, 6H, $\mathrm{P(CH(C}H_3\mathrm{)_2))}$, 0.73 (dd, 6H, $\mathrm{P(CH(C}H_3\mathrm{)_2))}$, –10.80 (br, 1H, B–H···Ru). **^{11}B{^{1}H}** ($\mathrm{C_6D_6}$): δ 6.18 ($B\mathrm{(BH_3)}$), -0.5 (*B*Ru), -9.5 (*B*H), -11.8 (*B*H), -14.9 (*B*H), -17.1 (*B*H), -49.9 ($\mathrm{B(}B\mathrm{H_3)}$). **^{13}C** ($\mathrm{C_6D_6}$): δ 104.8 ($C_2\mathrm{B_{10}}$), 35.7 ($\mathrm{P(}C\mathrm{H(CH_3)_2)}$, 29.8($\mathrm{P(}C\mathrm{H(CH_3)_2)}$, 20.5 ($\mathrm{P(CH(}C\mathrm{H_3)_2)}$, 18.8 ($\mathrm{P(CH(}C\mathrm{H_3)_2)}$, 15.2 ($\mathrm{P(CH(}C\mathrm{H_3)_2)}$. **^{31}P{^{1}H}** ($\mathrm{C_6D_6}$): δ 206.9. Selected bands in the IR spectrum, cm^{-1}: 2970–2870 (br, CH), 2600 (br, BH), 2418, 2388, 2008 (br, BH), 2034 (strong, Ru-CO), 1992 (strong, Ru-CO). Found: C, 32.82; H, 6.46. Calcd. for $\mathrm{C_{16}H_{39}B_{11}O_4P_2Ru}$: C, 33.16; H, 6.78.

References:

1. Eleazer, B. J.; Smith, M. D.; Peryshkov, D. V. *Organometallics*, **2016**, *35*, 106–112.

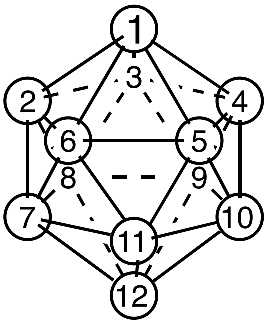

Figure S-5. The numbering scheme for the icosahedral *closo*-carborane cluster. For the *m*-$C_2B_{10}H_{12}$, carbon atoms are at positions 1 and 7. In the BB-carboryne complex of ruthenium (POBBOP)Ru$(CO)_2$ (**2**), the boron atoms at positions 2 and 6 are metalated.

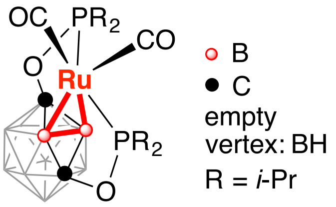

2

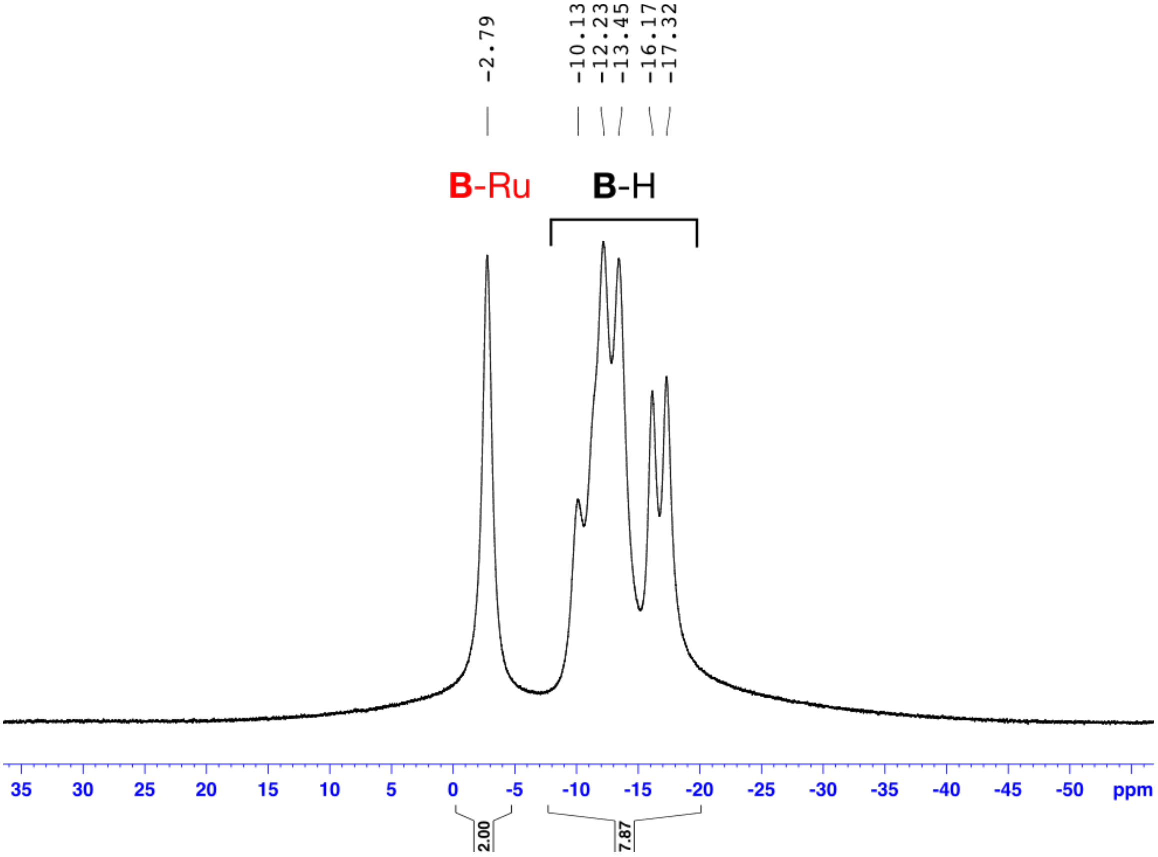

Figure S-6. The ^{11}B NMR spectrum of the ruthenium BB-carboryne complex (POBBOP)Ru(CO)$_2$ (**2**) in C_6D_6.

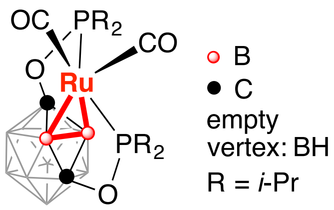

2

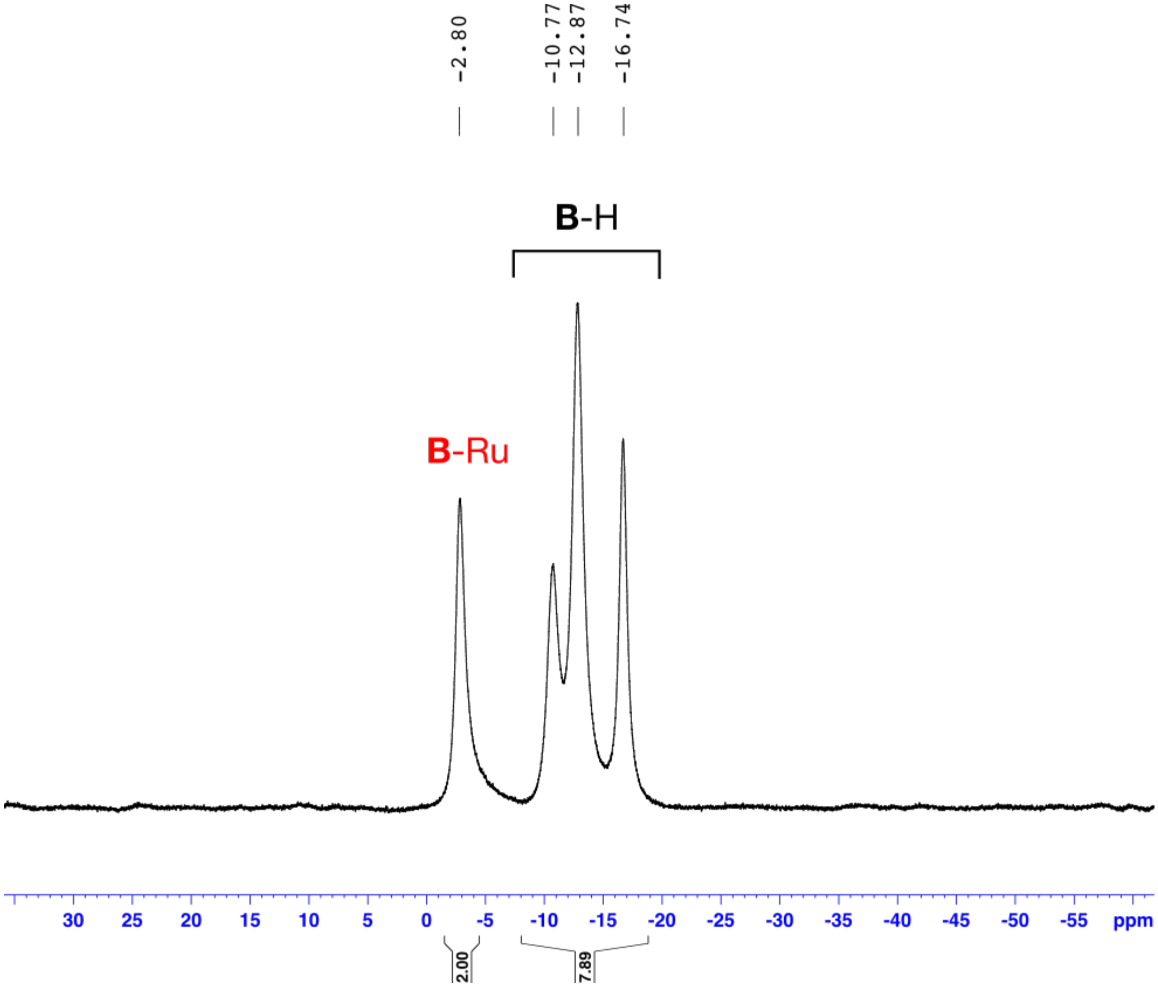

Figure S-7. The $^{11}B\{^{1}H\}$ NMR spectrum of the ruthenium BB-carboryne complex (POBBOP)Ru(CO)$_2$ (**2**) in C_6D_6.

$^{11}B\{^{1}H\}$ (C_6D_6): δ -2.8 (*B*-Ru), -10.8 (*B*-H), -12.9 (*B*-H), -16.7 (*B*-H).

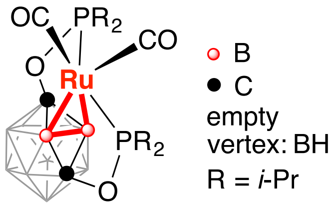

2

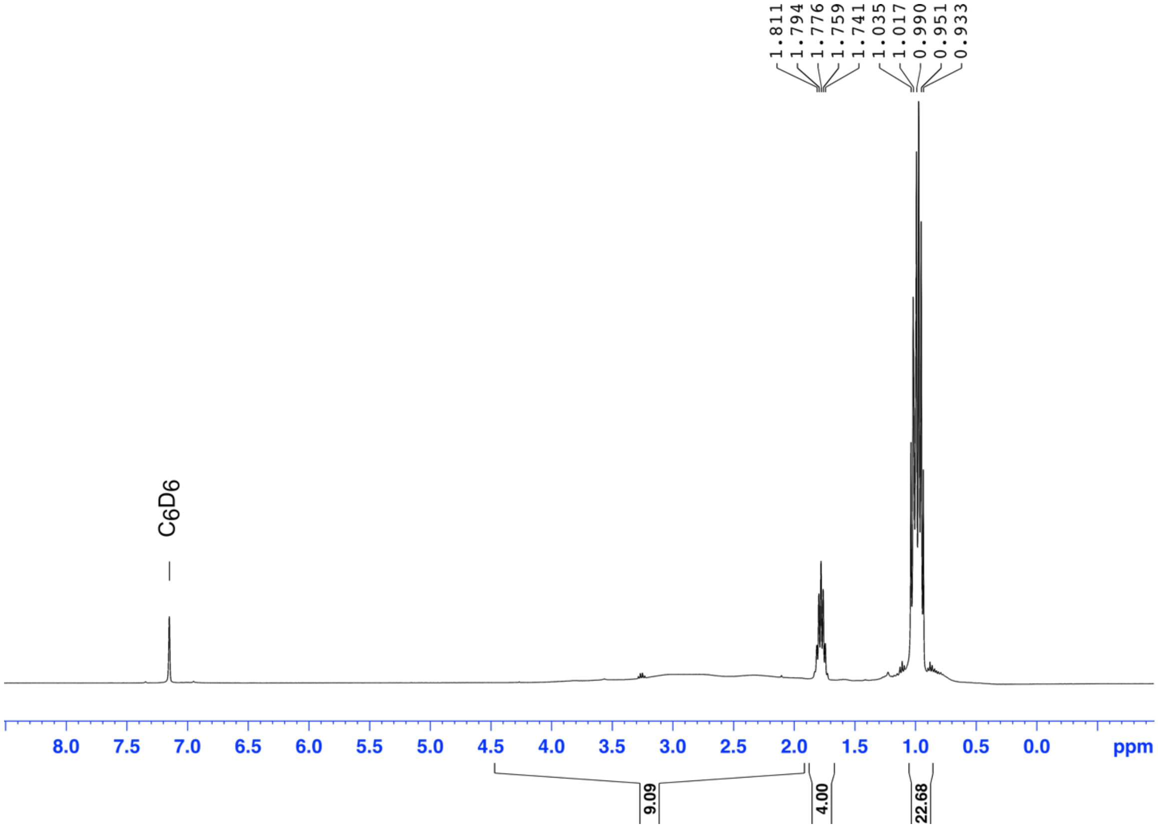

Figure S-8. The ^{1}H NMR spectrum of the ruthenium BB-carboryne complex (POBBOP)Ru(CO)$_2$ (**2**) in C_6D_6.

^{1}H (C_6D_6): δ 4.5–1.5 (br m, 8H, B*H*), 1.80 (m, 4H, P(C*H*(CH$_3$)$_2$), 1.00 (m, 24H, P(CH(C*H*$_3$)$_2$).

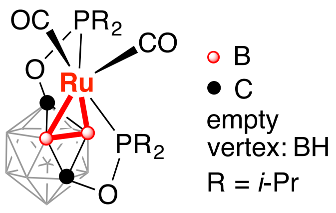

2

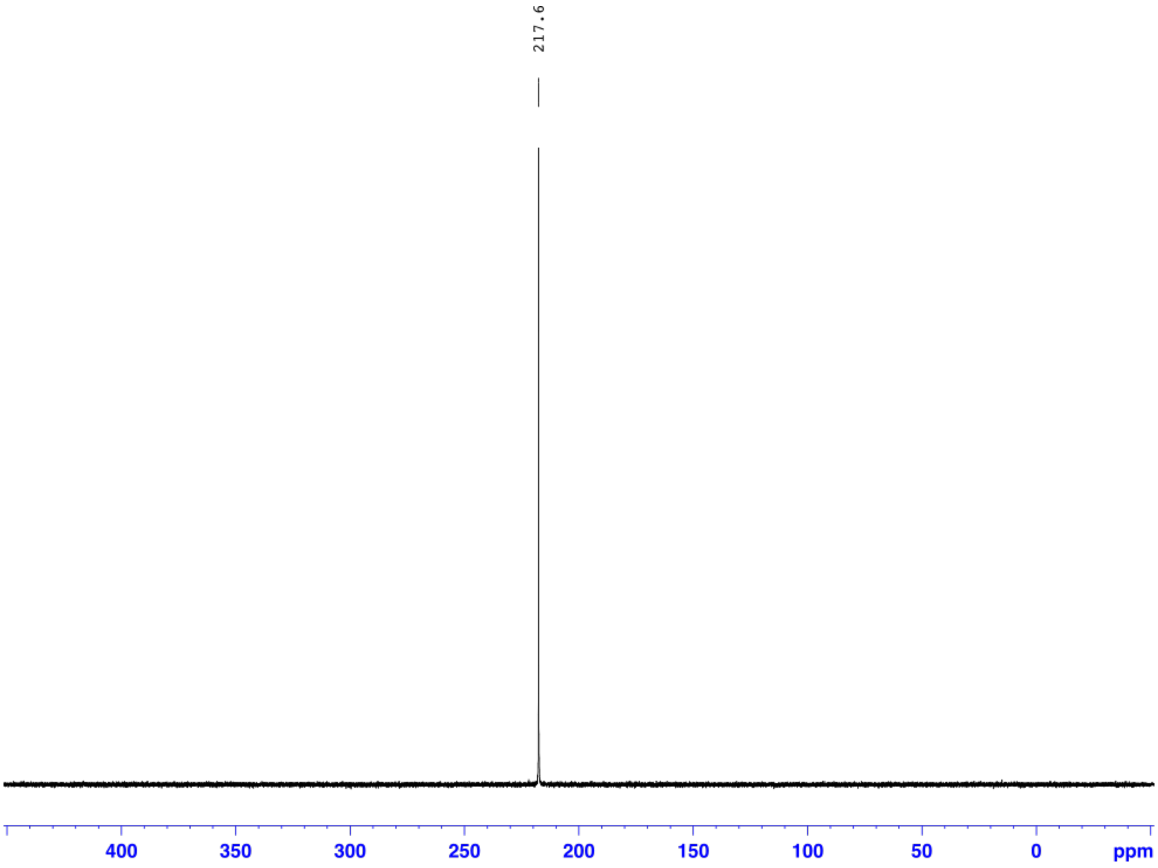

Figure S-9. The ^{31}P NMR spectrum of the ruthenium BB-carboryne complex (POBBOP)Ru(CO)$_2$ (**2**) in C_6D_6.

^{31}P (C_6D_6): δ 217.6.

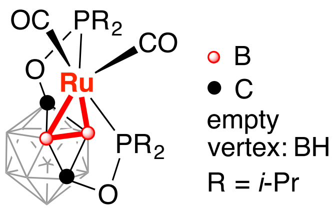

2

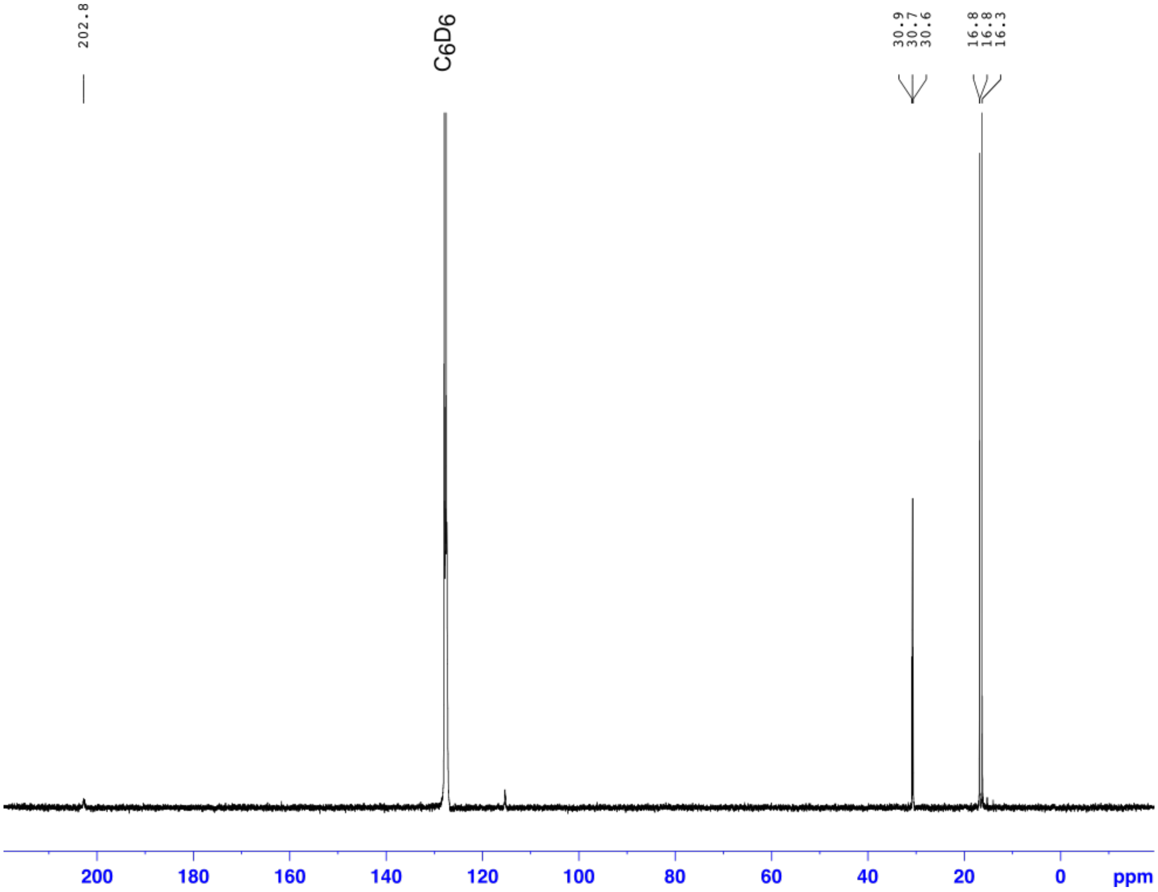

Figure S-10. The ^{13}C NMR spectrum of the ruthenium BB-carboryne complex (POBBOP)Ru(CO)$_2$ (**2**) in C_6D_6.

^{13}C (C_6D_6): δ 202.8 (Ru-*C*O), 115.3 ($C_2B_{10}H_8$), 30.7 (P(*C*H(CH$_3$)$_2$), 16.8 (P(CH(*C*H$_3$)$_2$).

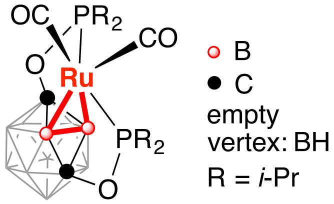

2

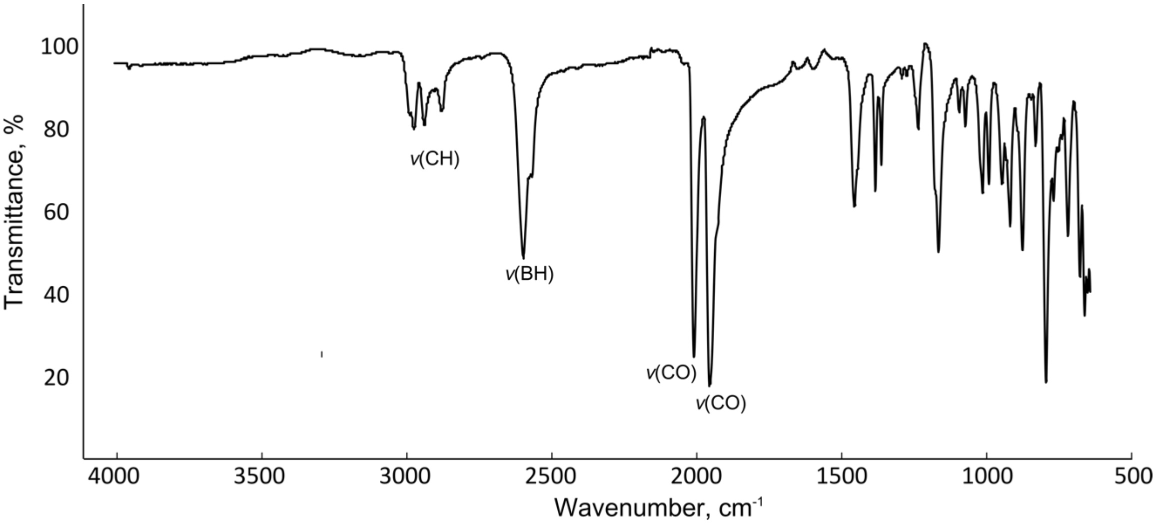

Figure S-11. The ATR-FTIR absorption spectrum of a solid sample of the ruthenium BB-carboryne complex (POBBOP)Ru(CO)$_2$ (**2**)

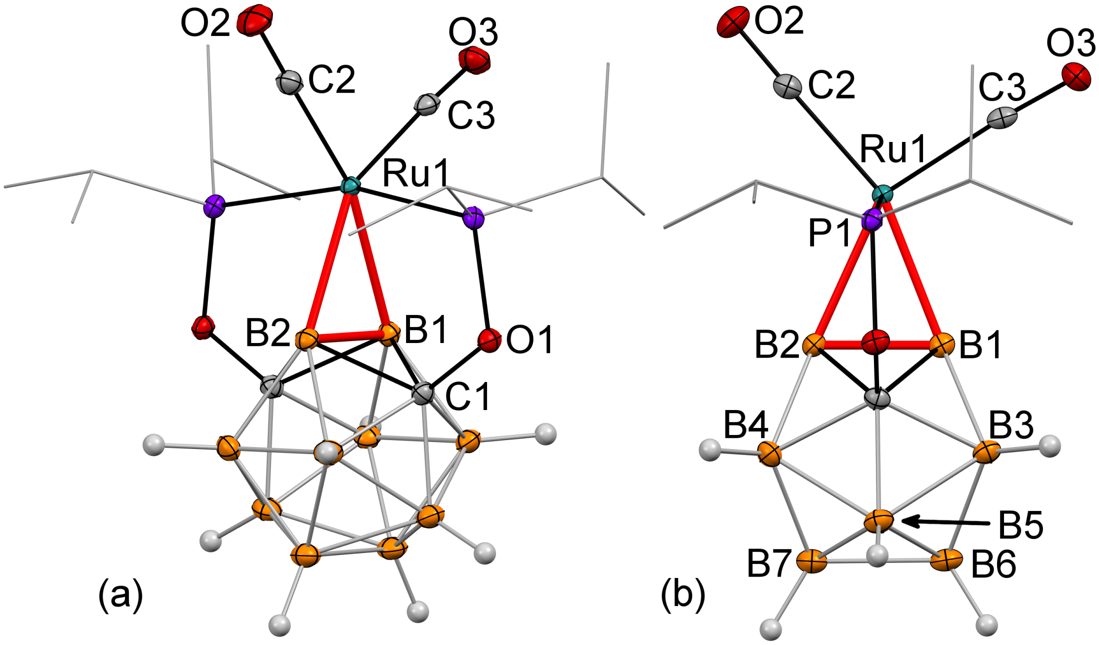

Figure S-12. Displacement ellipsoid plot (50% probability) of the (POBBOP)Ru(CO)$_2$ complex (POBBOP = 1,7-OP(*i*-Pr)$_2$-2,6-dehydro-*m*-carborane) (**2**). (a): a general view (b): a view perpendicular to the (B1–B2–Ru1–C2–C3) plane. Atoms belonging to isopropyl groups of the ligand arms have been omitted for clarity. Selected bond distances (Å) and angles (°): Ru1–B1 = 2.174(3), Ru1–B2 = 2.221(3), B1–B2 = 1.720(4), Ru1–C2 = 1.939(3) Ru1–C3 = 1.915(3), B2–B4 = 1.811(3), B1–B3 = 1.796(3), B4–B7 = 1.781(3), B3–B6 = 1.785(3), B7–B6 = 1.812(4), B2–B1–Ru1 = 68.4(1), B1–B2–Ru1 = 65.5(1), and C2–Ru1–C3 = 98.6(1).

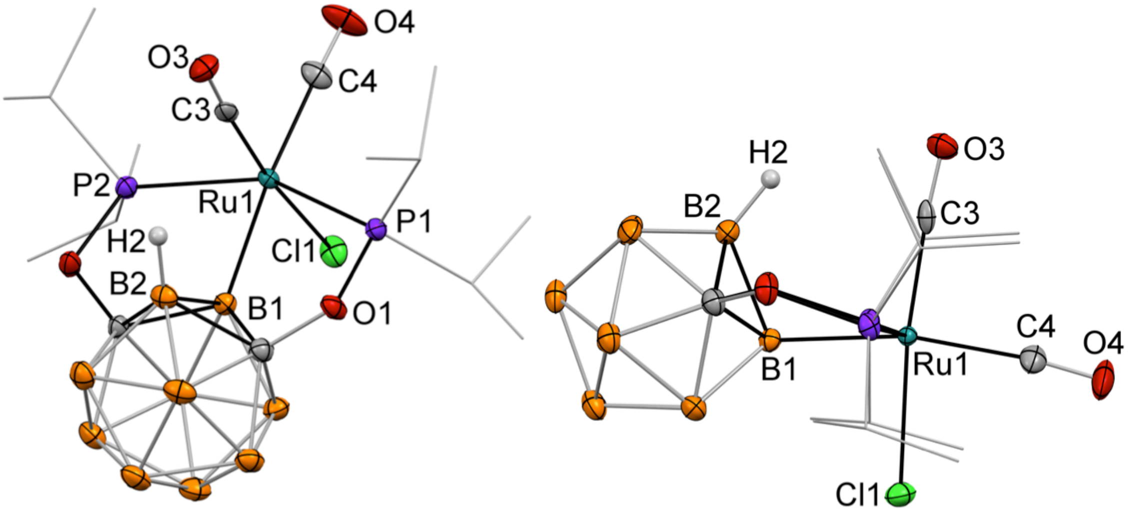

Figure S-13. Displacement ellipsoid plots (50% probability) of (POBOP)Ru(Cl)(CO)$_2$ (**3**). (left): a general view (right): a view perpendicular to the (B2–B1–Ru1–C4) plane. Atoms belonging to isopropyl groups of the ligand arms and all hydrogen atoms except H2 have been omitted for clarity.

Selected bond distances (Å) and angles (°): Ru1–B1 = 2.125(3), Ru1–C3 = 1.856(3), Ru1–C4 = 1.972(3), Ru1–Cl1 = 2.449(8), B1–B2 = 1.791(5), B2–B1–Ru1 = 109.7(2), B1–Ru1–C4 = 167.4(1), C3–Ru1–Cl1 = 173.5(1).

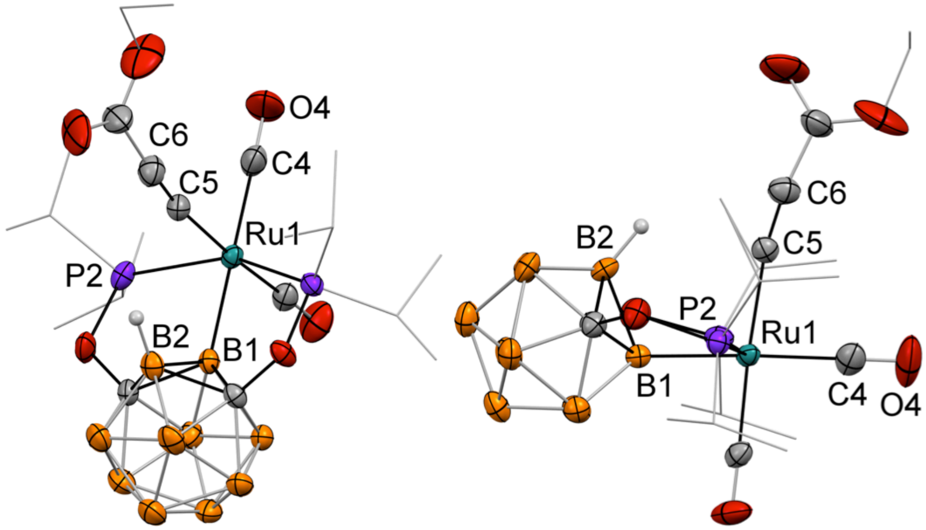

Figure S-14. Displacement ellipsoid plots (50% probability) of (POBOP)Ru(C≡CCO$_2$Et)(CO)$_2$ (**4**). (left): a general view (right): a view perpendicular to the (B2–B1–Ru1–C4) plane. Atoms belonging to isopropyl groups of the ligand arms and the ester group and all hydrogen atoms except one connected to B2 have been omitted for clarity.

Selected bond distances (Å) and angles (°): Ru1–B1 = 2.121(3), Ru1–C5 = 2.062(3), B1–B2 = 1.793(5), C5–C6 = 1.199(5), B2–B1–Ru1 = 110.6(2), Ru1–C5–C6 = 171.3(3).

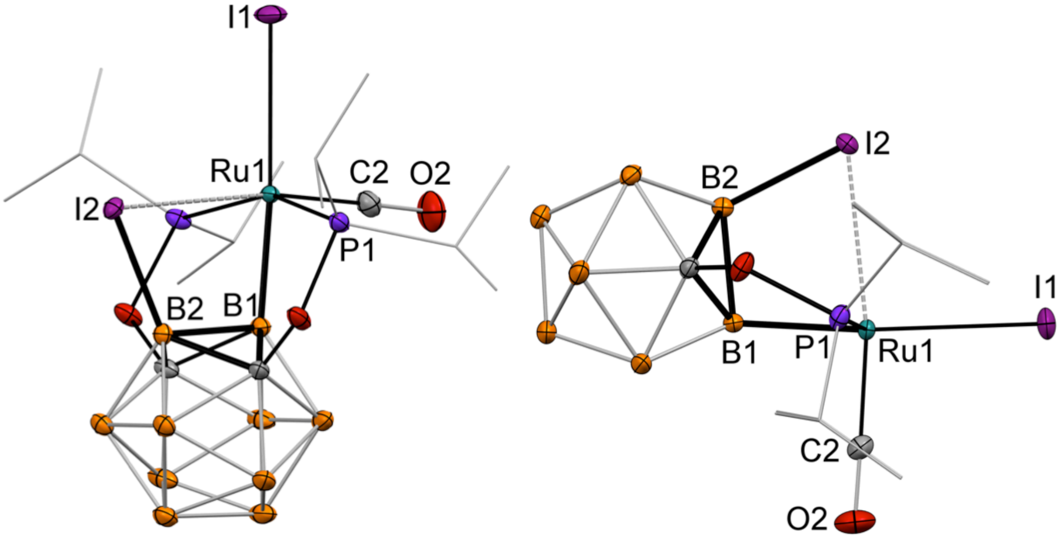

Figure S-15. Displacement ellipsoid plots (50% probability) of (POBB(I)OP)Ru(I)(CO) (**5**). (left): a general view (right): a view perpendicular to the (B2–B1–Ru1–I1) plane. Atoms belonging to isopropyl groups of the ligand arms and all hydrogen atoms have been omitted for clarity.

Selected bond distances (Å) and angles (°): Ru1–B1 = 2.059(2), Ru1–I1 = 2.777(1), Ru1–I1 = 2.884(1), B1–B2 = 1.791(3), Ru1–C2 = 1.819(2), B2–I2 = 2.156(2), B2–B1–Ru1 = 98.2(1), B1–Ru1–I1 = 175.2(6), and I2–Ru1–C2 = 170.9(1).

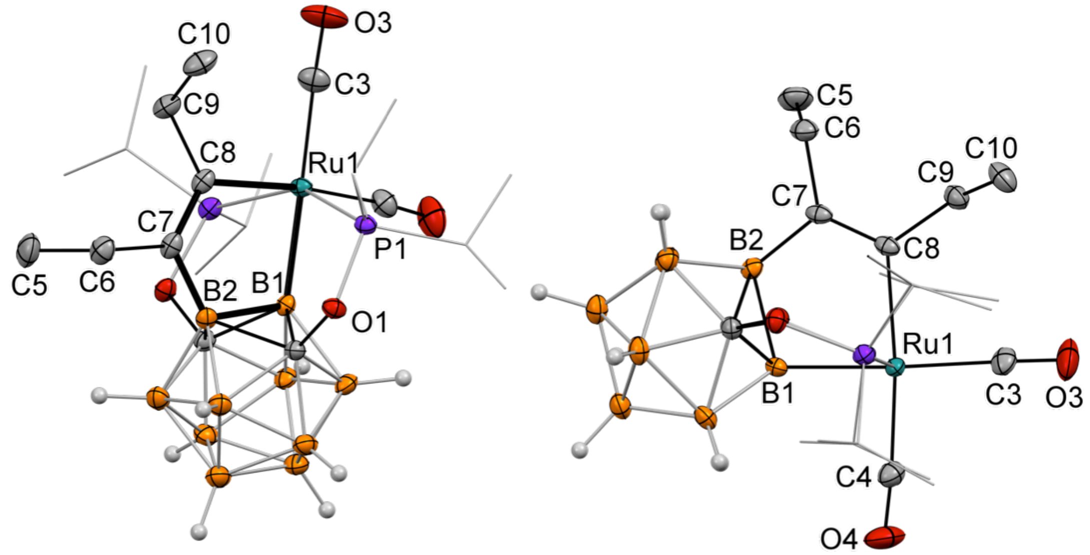

Figure S-16. Displacement ellipsoid plots (50% probability) of (POBOP)(EtC=CEt)Ru(CO)$_2$ (**6**). (left): a general view (right): a view perpendicular to the (B2–B1–Ru1–C4) plane. Atoms belonging to isopropyl groups of the ligand arms and all hydrogen atoms except those on the boron cage have been omitted for clarity. Selected bond distances (Å) and angles (°): Ru1–B1 = 2.123(2), Ru1–C8 = 2.172(2), B1–B2 = 1.815(4), B2–C7 = 1.542(4), C7–C8 = 1.343(3), B2–B1–Ru1 = 104.0(1), B1–B2–C7 = 115.0(2).

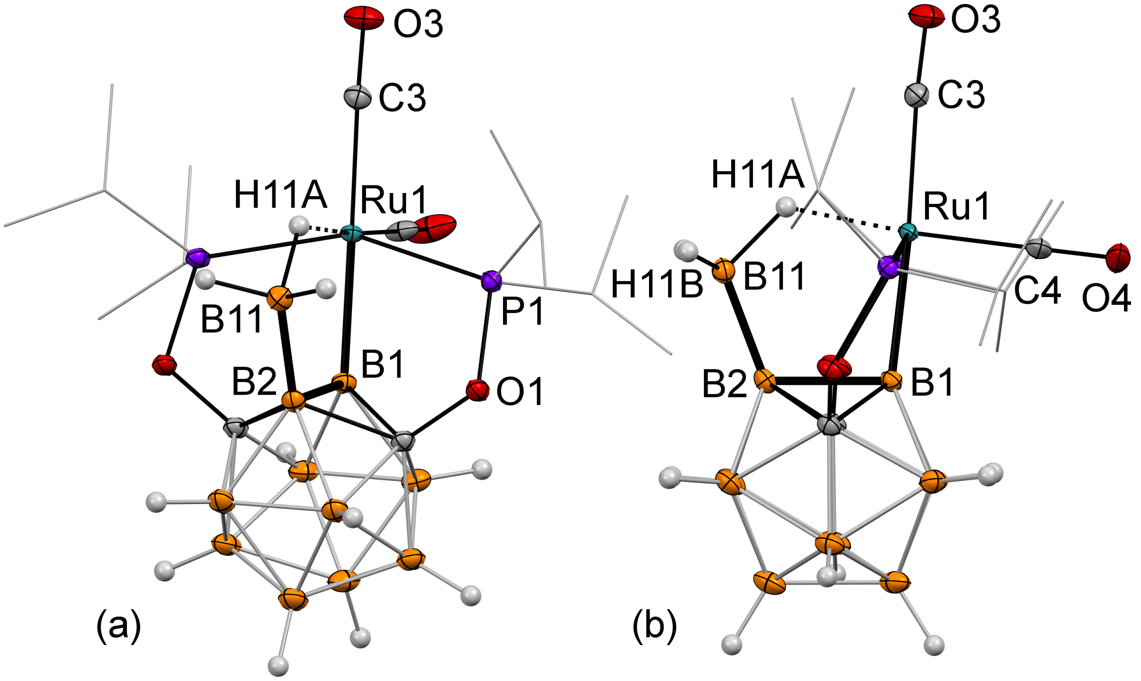

Figure S-17. Displacement ellipsoid plot (50% probability) of the (POB(BH$_3$)OP)Ru(CO)$_2$ complex (**7**). (a): a general view (b): a view perpendicular to the (B2–B1–Ru1–C3–C4) plane. Atoms belonging to isopropyl groups of the ligand arms have been omitted for clarity. Selected bond distances (Å) and angles (°): Ru1–B1 = 2.136(1), B1–B2 = 1.803(1), B2–B11 = 1.680(1), Ru1···H11A = 1.79(1), B11–H11A = 1.28(1), B11–H11B = 1.09(1), B2–B1–Ru1 = 95.6(1), B1–B2–B11 = 110.8(1), and B1–Ru1–C3 = 176.8(1), and H11A···Ru1–C4 = 174.8(4).

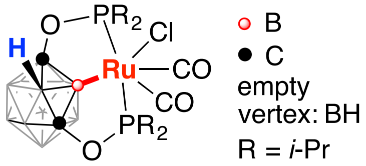

3

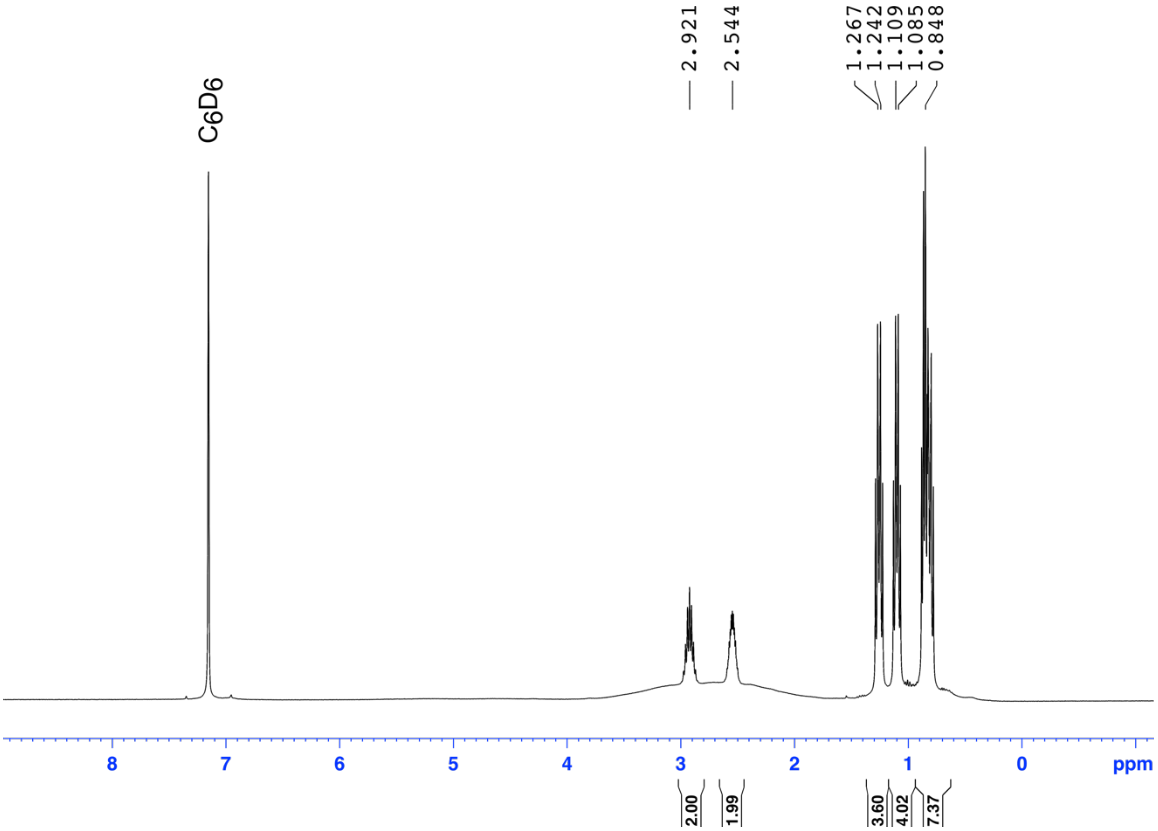

Figure S-18. The ^{1}H NMR spectrum of (POBOP)Ru(Cl)(CO)$_2$ (**3**) in C_6D_6.

^{1}H NMR (C_6D_6): δ 4.00–1.50 (br, 9H, $C_2B_{10}H_9$), 2.92 (m, 2H, P(C*H*(CH$_3$)$_2$), 2.54 (m, 2H, P(C*H*(CH$_3$)$_2$) 1.25 (dd, 6H, P(CH(C*H*$_3$)$_2$)), 1.09 (dd, 6H, P(CH(C*H*$_3$)$_2$)), 0.84 (dd, 12H, P(CH(C*H*$_3$)$_2$)).

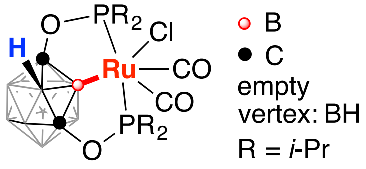

3

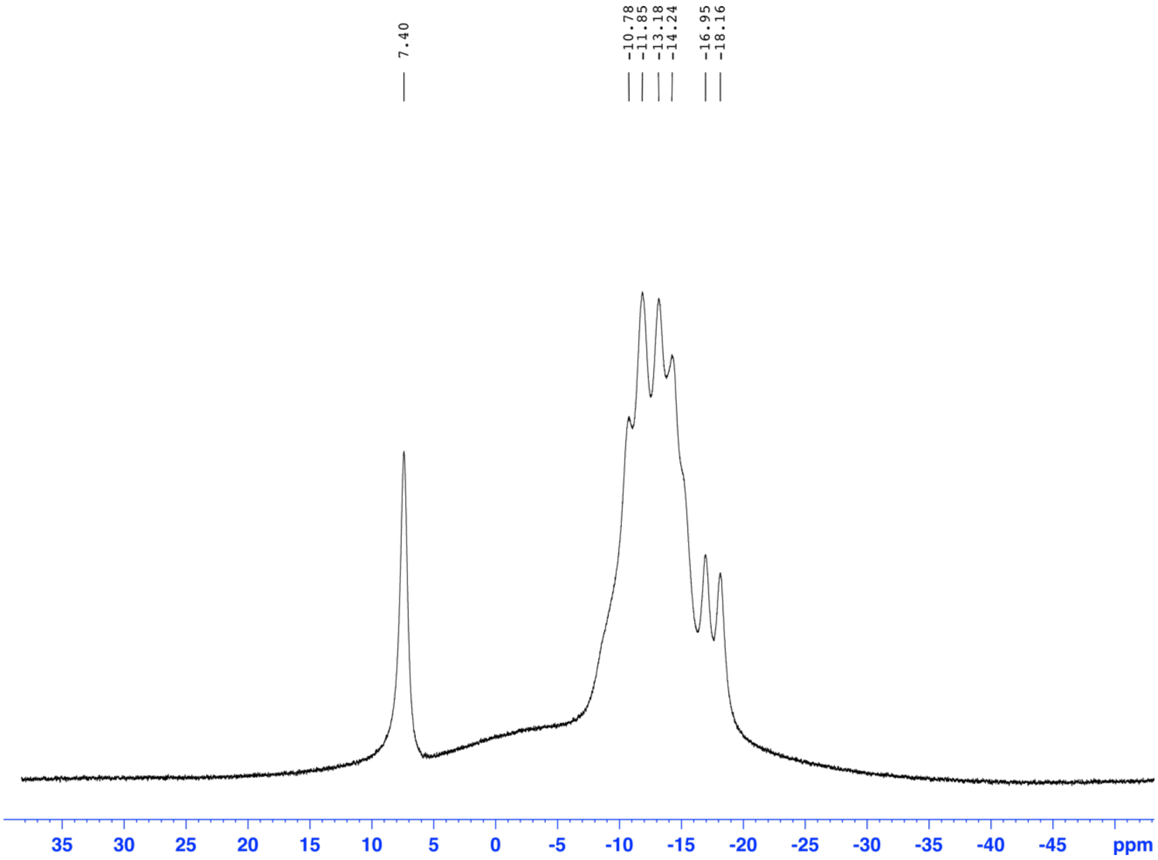

Figure S-19. The ^{11}B NMR spectrum of (POBOP)Ru(Cl)$(CO)_2$ (**3**) in C_6D_6.

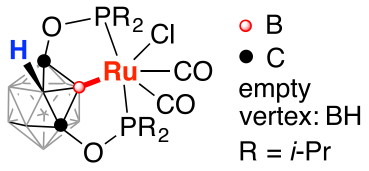

3

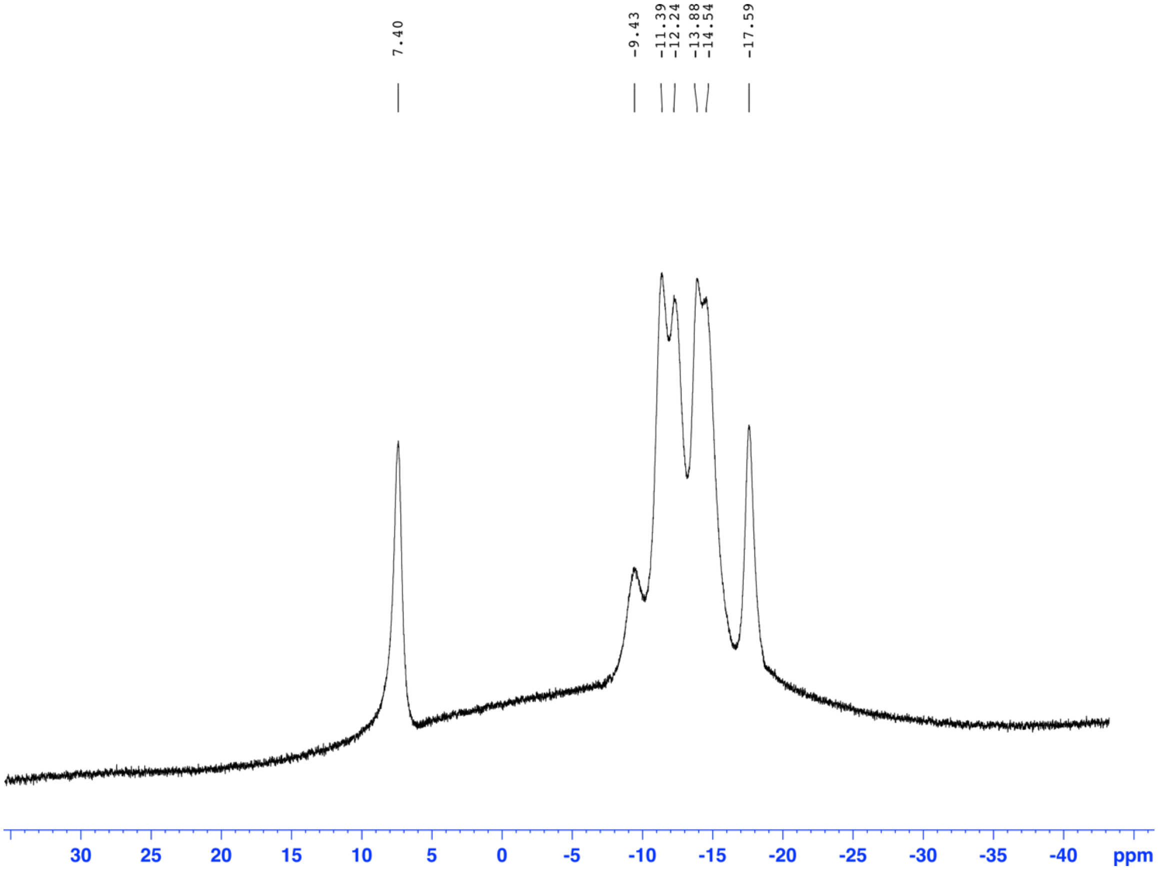

Figure S-20. The $^{11}B\{^1H\}$ NMR spectrum of (POBOP)Ru(Cl)(CO)$_2$ (**3**) in C_6D_6.

$^{11}B\{^1H\}$ (C_6D_6): δ 7.4 (s, *B*Ru), –9.4 (*B*H), –11.4 (*B*H), –12.2 (*B*H), –13.8 (*B*H), –14.5 (*B*H), –17.6 (*B*H).

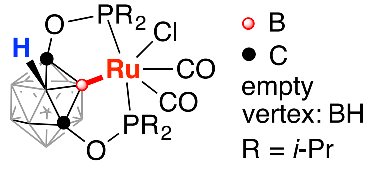

3

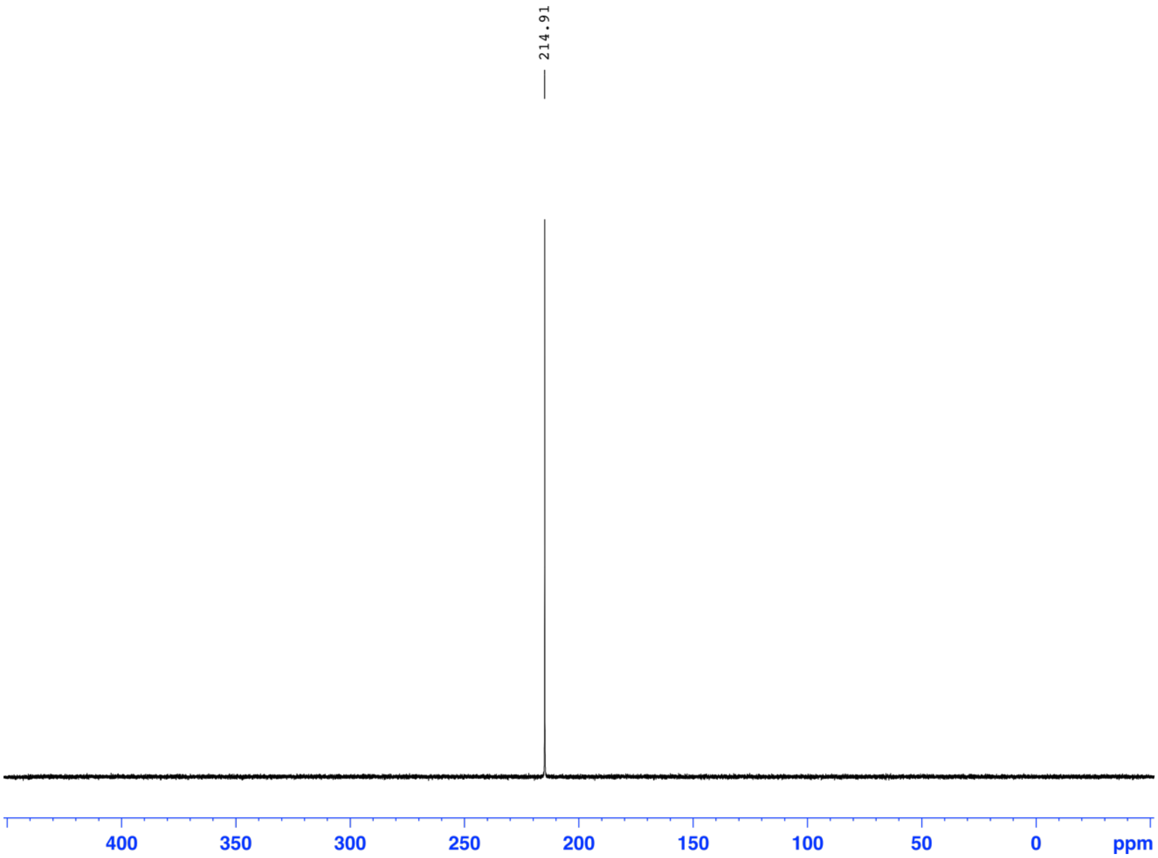

Figure S-21. The ^{31}P NMR spectrum of (POBOP)Ru(Cl)(CO)$_2$ (**3**) in C_6D_6.

^{31}P (C_6D_6): δ 214.9.

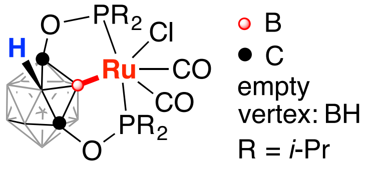

3

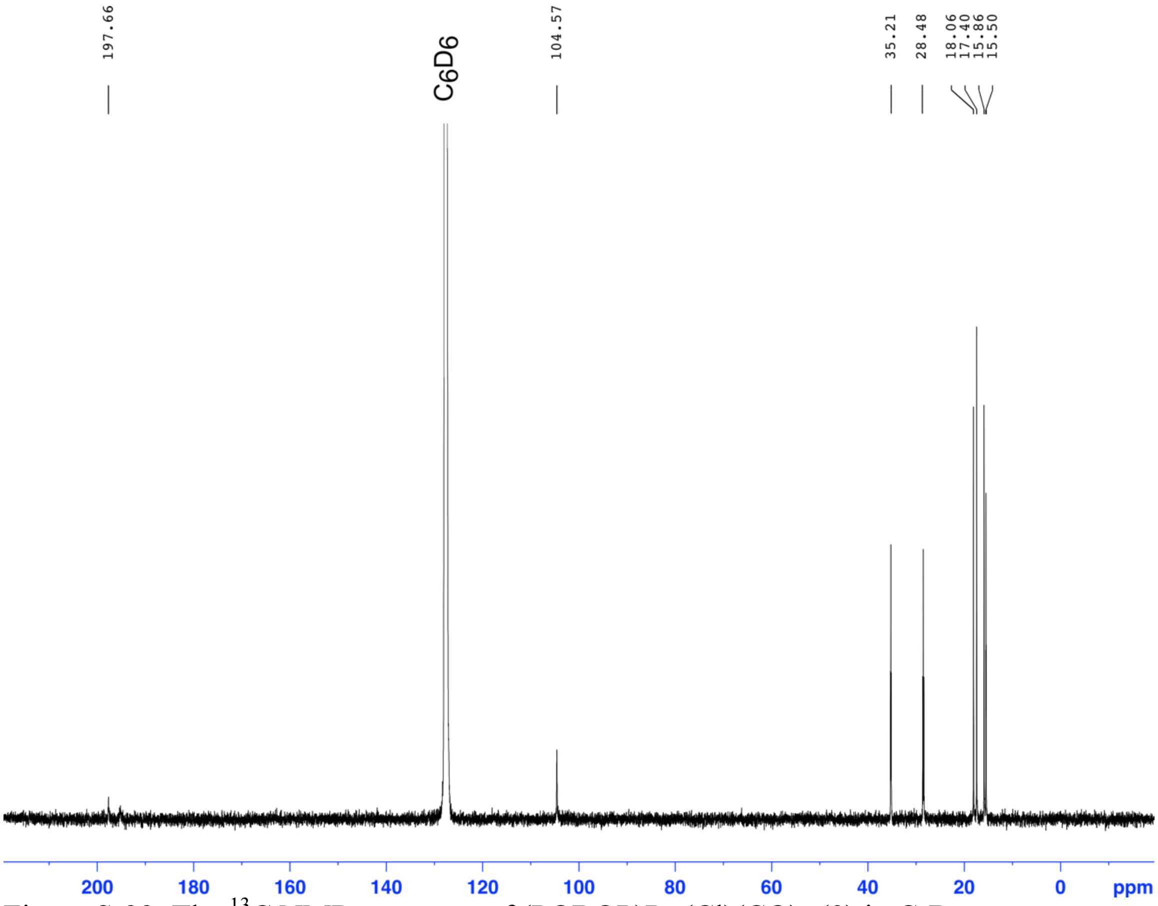

Figure S-22. The ^{13}C NMR spectrum of (POBOP)Ru(Cl)(CO)$_2$ (**3**) in C_6D_6.

^{13}C (C_6D_6): δ 197.7 (Ru-*C*O), 196.4 (Ru-*C*O), 104.6 (*C*$_2$B$_{10}$), 35.2 (P(*C*H(CH$_3$)$_2$), 28.5 (P(*C*H(CH$_3$)$_2$), 17.6 (P(CH(*C*H$_3$)$_2$), 15.5 (P(CH(*C*H$_3$)$_2$).

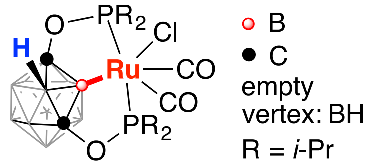

3

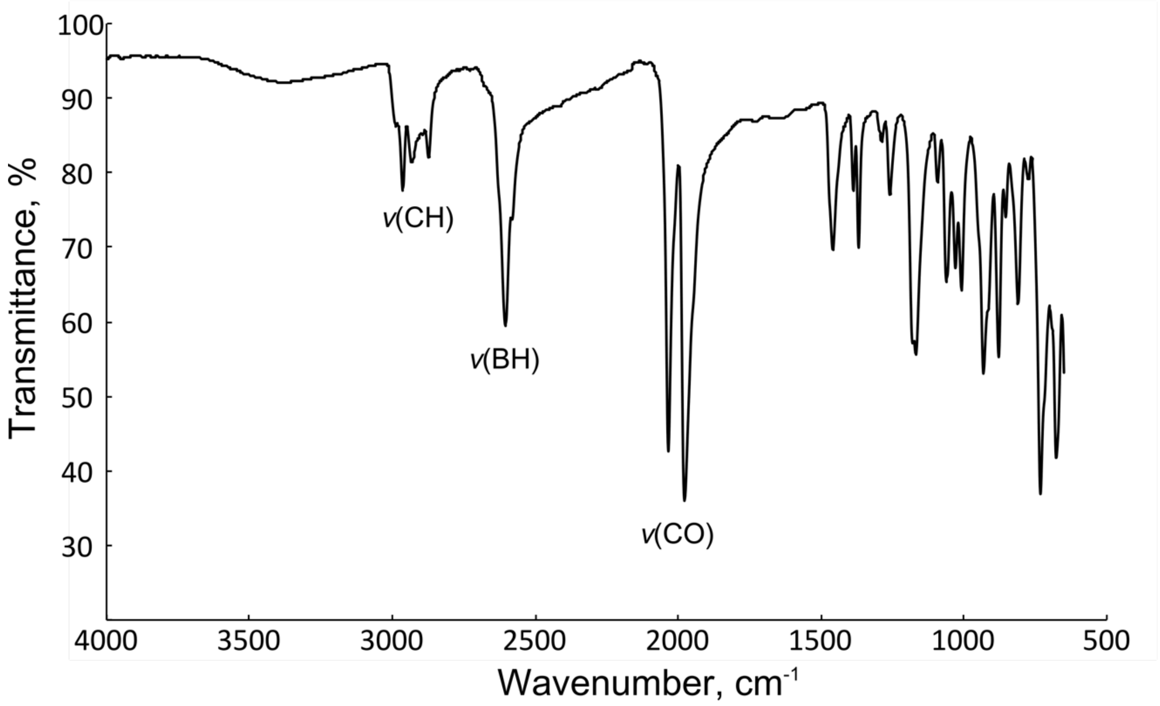

Figure S-23. The ATR-FTIR absorption spectrum of a solid sample of (POBOP)Ru(Cl)$(CO)_2$ (**3**)

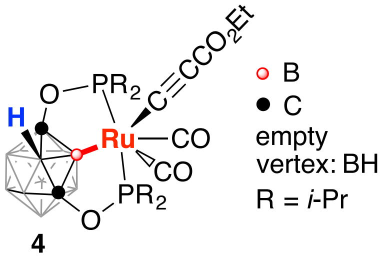

4

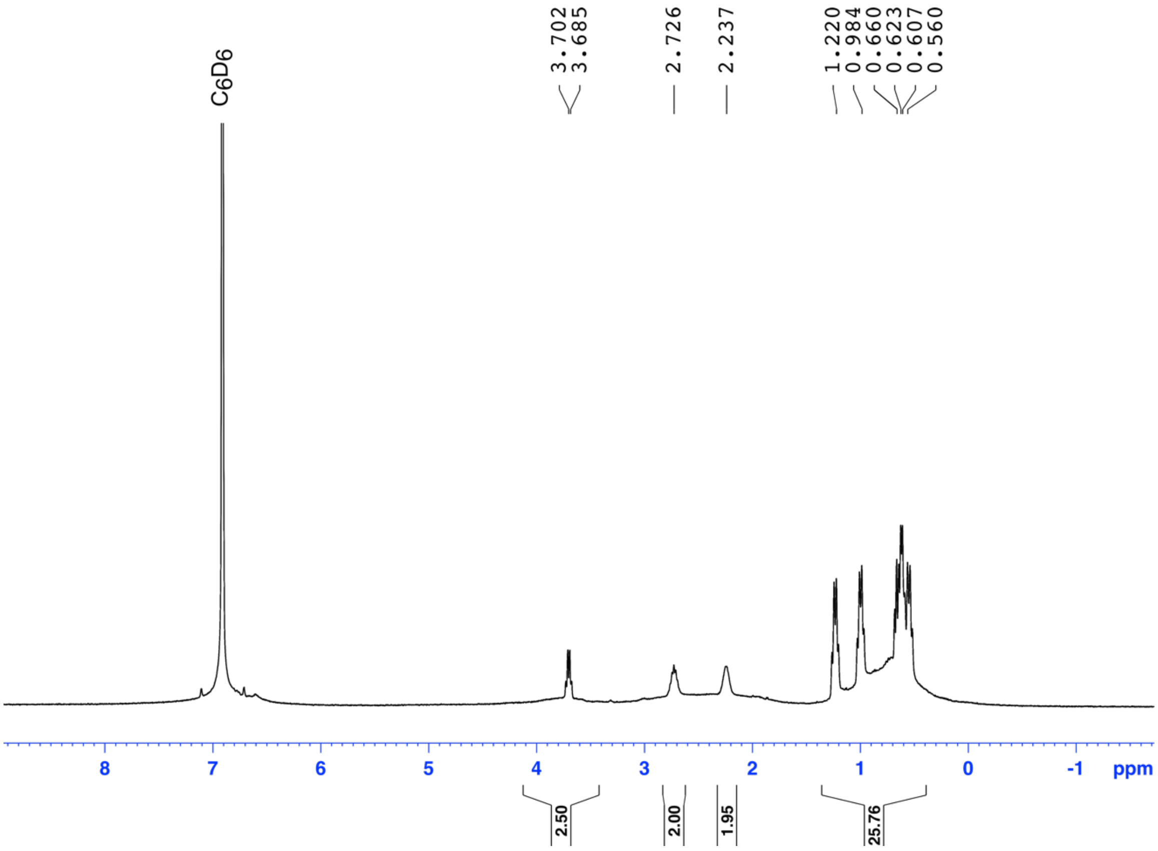

Figure S-24. The ^{1}H NMR spectrum of (POBOP)Ru(C≡CCO$_2$Et)(CO)$_2$ (**4**) in C_6D_6.

^{1}H NMR (C_6D_6): δ 4.50–1.00 (br, 9H, $C_2B_{10}H_9$), 3.69 (q, 2H, $CO_2CH_2CH_3$), 2.72 (m, 2H, P(C*H*(CH$_3$)$_2$), 2.24 (m, 2H, P(C*H*(CH$_3$)$_2$) 1.22 (dd, 6H, P(CH(C*H*$_3$)$_2$)), 0.98 (dd, 6H, P(CH(C*H*$_3$)$_2$)), 0.62 (overlapping 12H, P(CH(C*H*$_3$)$_2$) and 3H, $CO_2CH_2CH_3$).

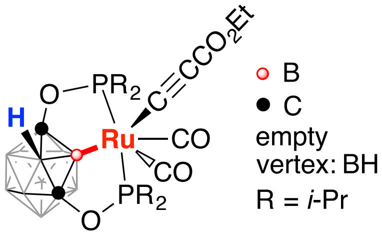

4

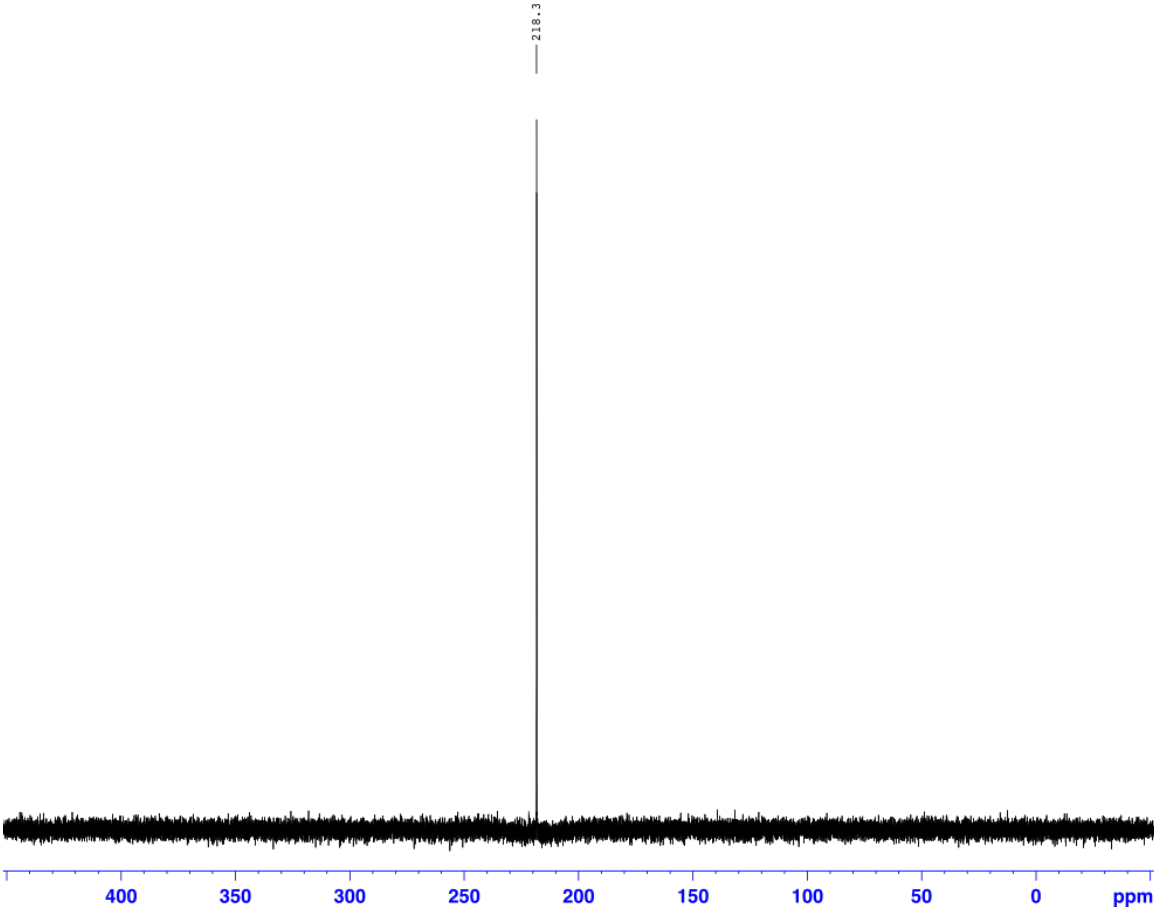

Figure S-25. The ^{31}P NMR spectrum of (POBOP)Ru(C≡CCO$_2$Et)(CO)$_2$ (**4**) in C_6D_6.

^{31}P NMR (C_6D_6): δ 218.3

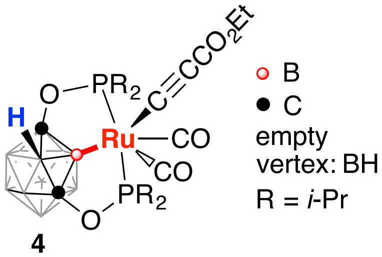

4

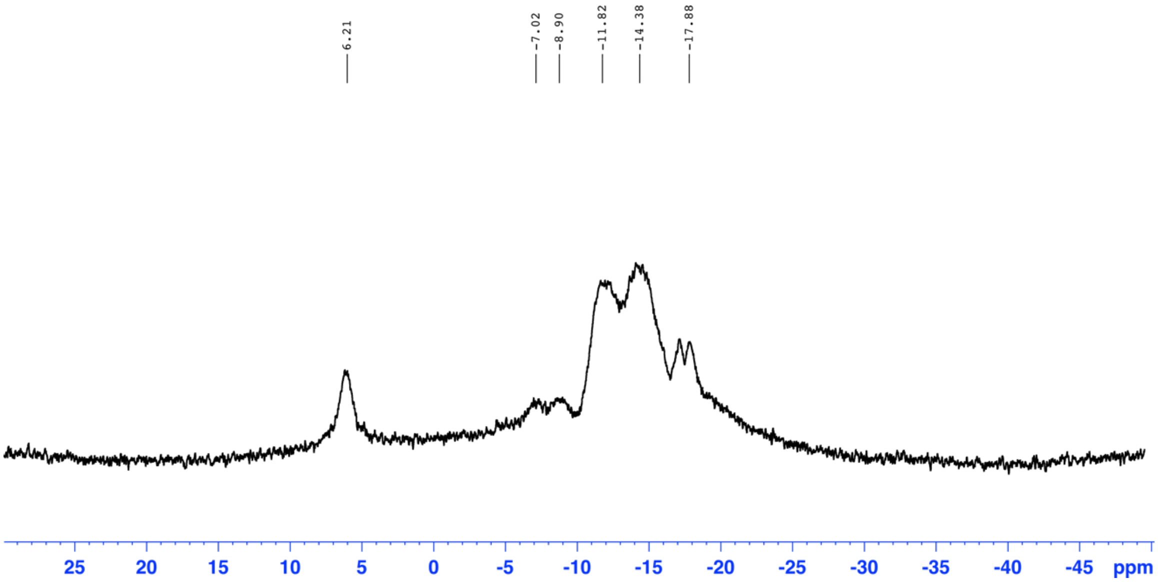

Figure S-26. The ^{11}B NMR spectrum of (POBOP)Ru(C≡CCO$_2$Et)(CO)$_2$ (**4**) in C$_6$D$_6$.

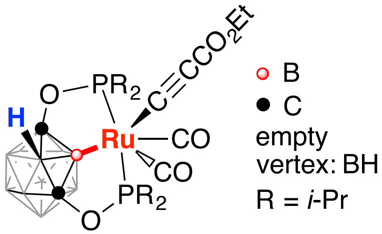

4

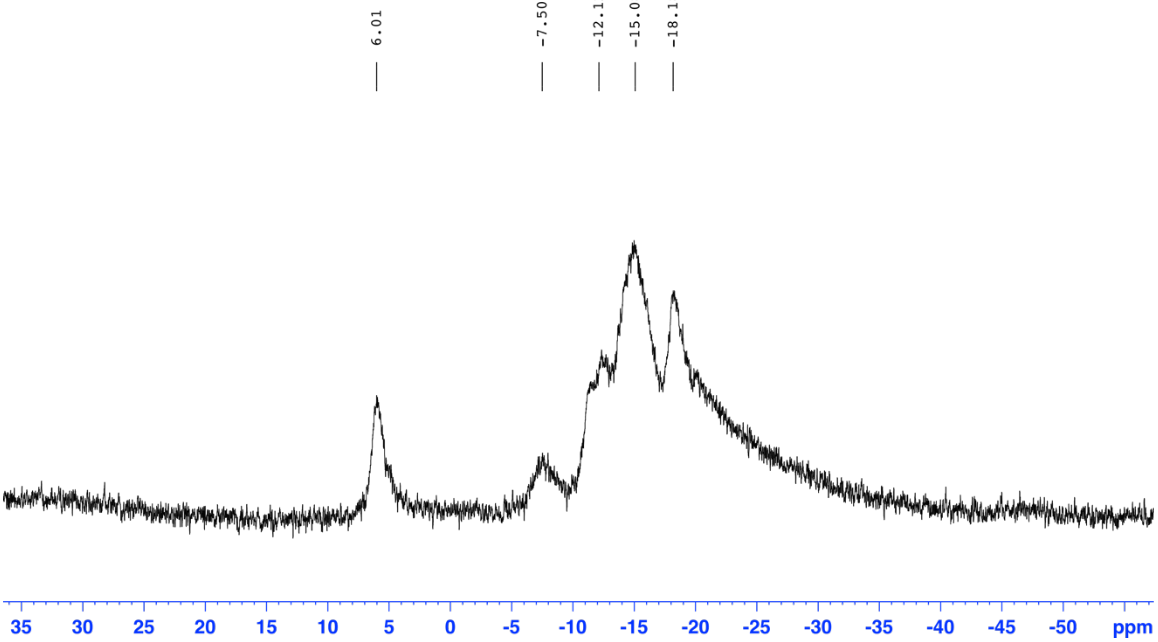

Figure S-27. The $^{11}B\{^1H\}$ NMR spectrum of (POBOP)Ru(C≡CCO_2Et)$(CO)_2$ (**4**) in C_6D_6.

$^{11}B\{^1H\}$ NMR (C_6D_6): δ 6.0 (*B*Ru), –7.5 to –18.8 (*B*H).

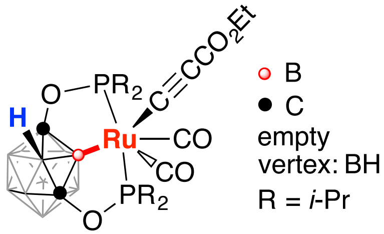

4

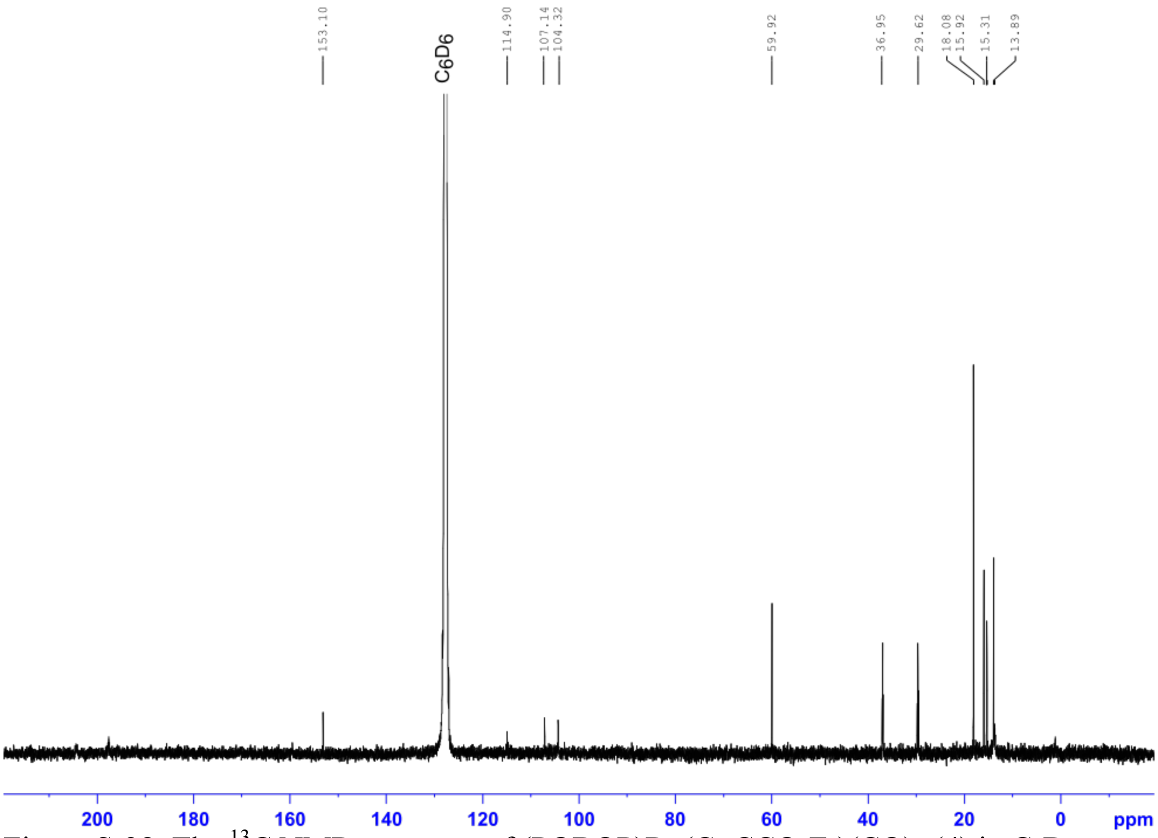

Figure S-28. The ^{13}C NMR spectrum of (POBOP)Ru(C≡CCO$_2$Et)(CO)$_2$ (**4**) in C_6D_6.

^{13}C (C_6D_6): δ 197.2 (Ru-*C*O), 153.1 (*C*≡*C*CO$_2$Et), 114.9 (*C*$_2$B$_{10}$), 107.14 (*C*≡*CC*O$_2$Et), 104.3 (*C*≡*CC*O$_2$Et), 59.9 (C≡CCO$_2$*C*H$_2$CH$_3$), 36.9 (P(*C*H(CH$_3$)$_2$), 29.6 (P(*C*H(CH$_3$)$_2$), 18.1 (C≡CCO$_2$CH$_2$*C*H$_3$), 15.9 (P(CH(*C*H$_3$)$_2$), 15.3 (P(CH(*C*H$_3$)$_2$), 13.8 (P(CH(*C*H$_3$)$_2$).

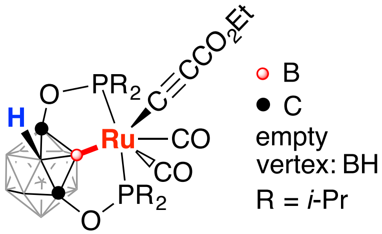

4

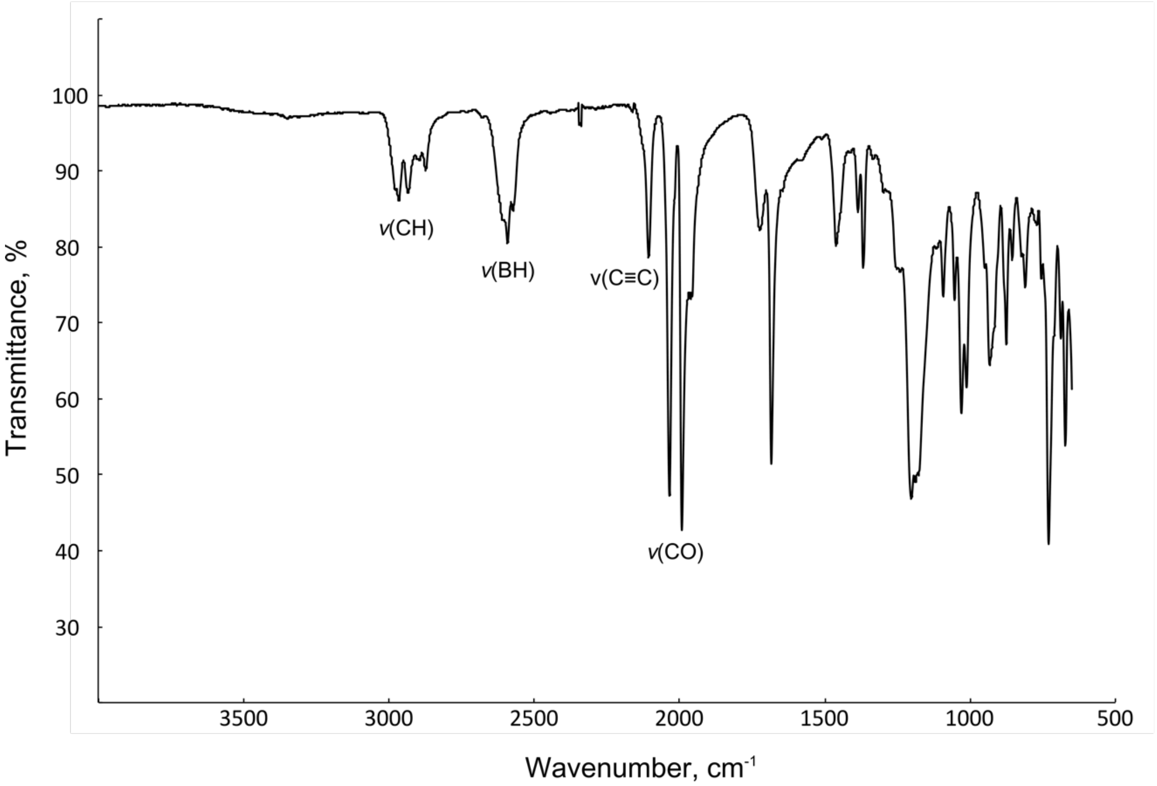

Figure S-29. The ATR-FTIR absorption spectrum of a solid sample of (POBOP)Ru(C≡CCO_2Et)$(CO)_2$ (**4**).

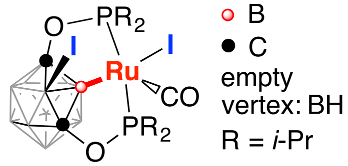

5

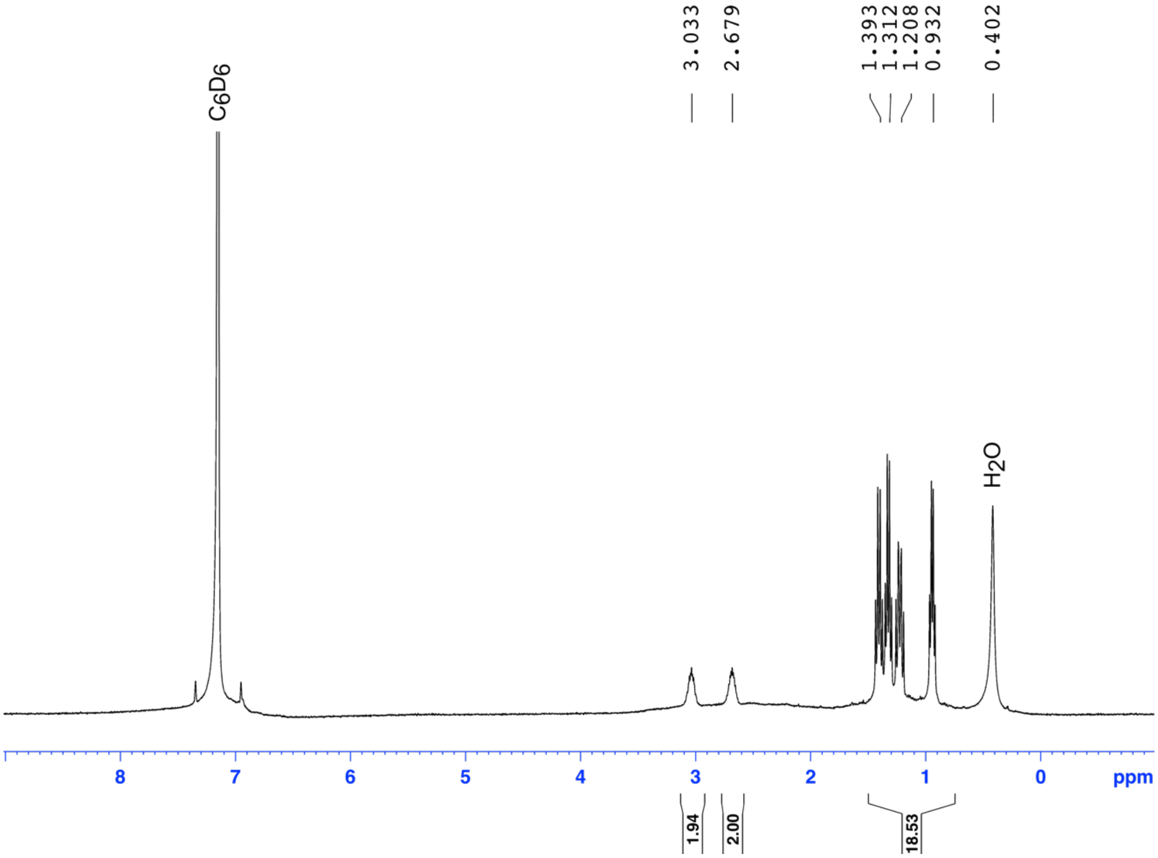

Figure S-30. The ^{1}H NMR spectrum of (POB(I)OP)Ru(I)(CO) (**5**) in C_6D_6.

^{1}H NMR (C_6D_6): δ 4.00–1.00 (br, 9H, $C_2B_{10}\mathit{H}_9$), 3.03 (m, 2H, P($C\mathit{H}(CH_3)_2$), 2.68 (m, 2H, P($C\mathit{H}(CH_3)_2$) 1.39 (dd, 6H, P($CH(C\mathit{H}_3)_2$)), 1.31 (dd, 6H, P($CH(C\mathit{H}_3)_2$)), 1.21 (dd, 6H, P($CH(C\mathit{H}_3)_2$)), 0.93 (dd, 6H, P($CH(C\mathit{H}_3)_2$)).

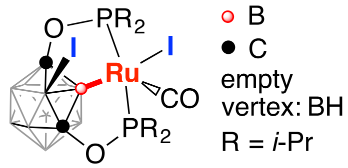

5

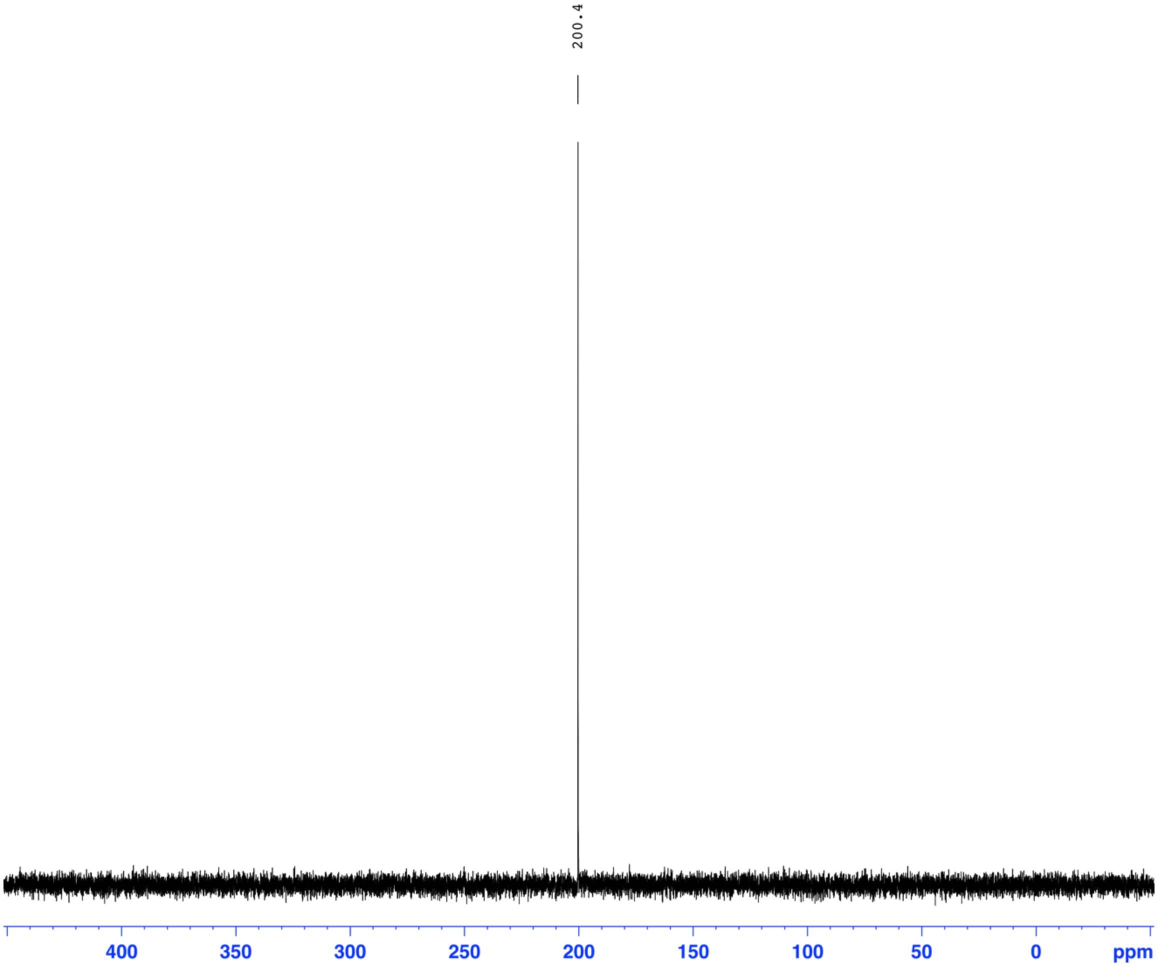

Figure S-31. The ^{31}P NMR spectrum of (POB(I)OP)Ru(I)(CO) (**5**) in C_6D_6.

^{31}P NMR (C_6D_6): δ 200.4

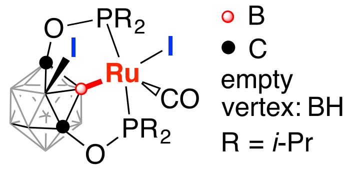

5

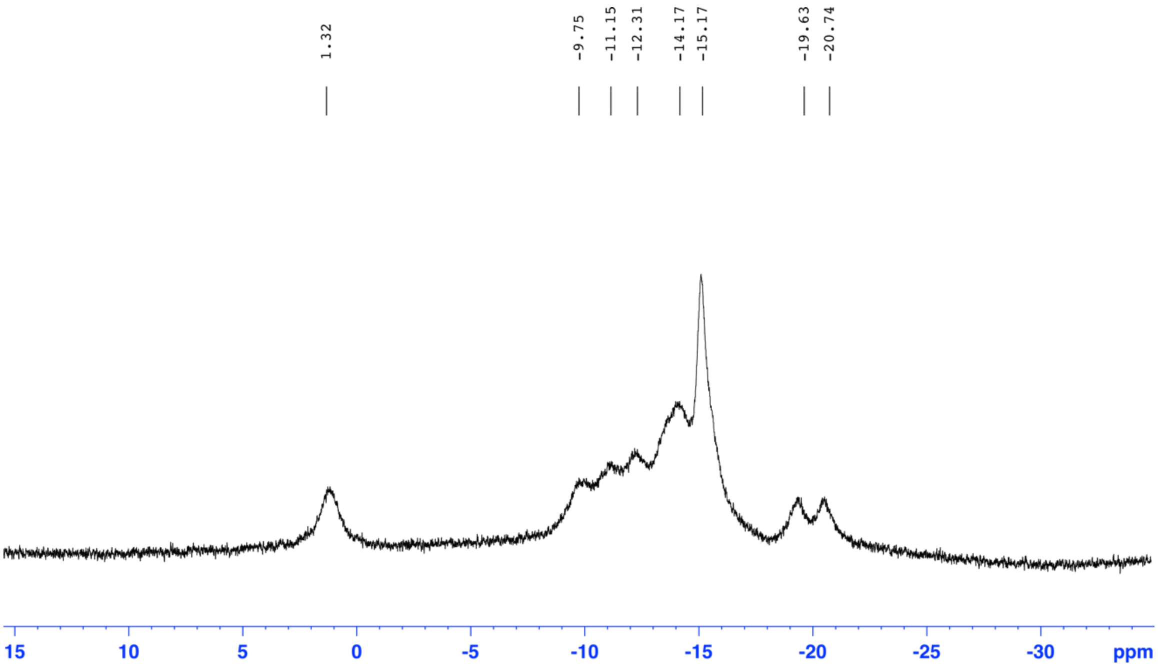

Figure S-32. The ^{11}B NMR spectrum of (POB(I)OP)Ru(I)(CO) (**5**) in C_6D_6.

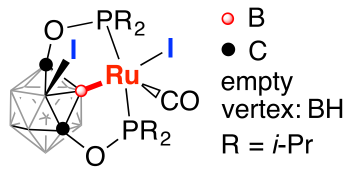

5

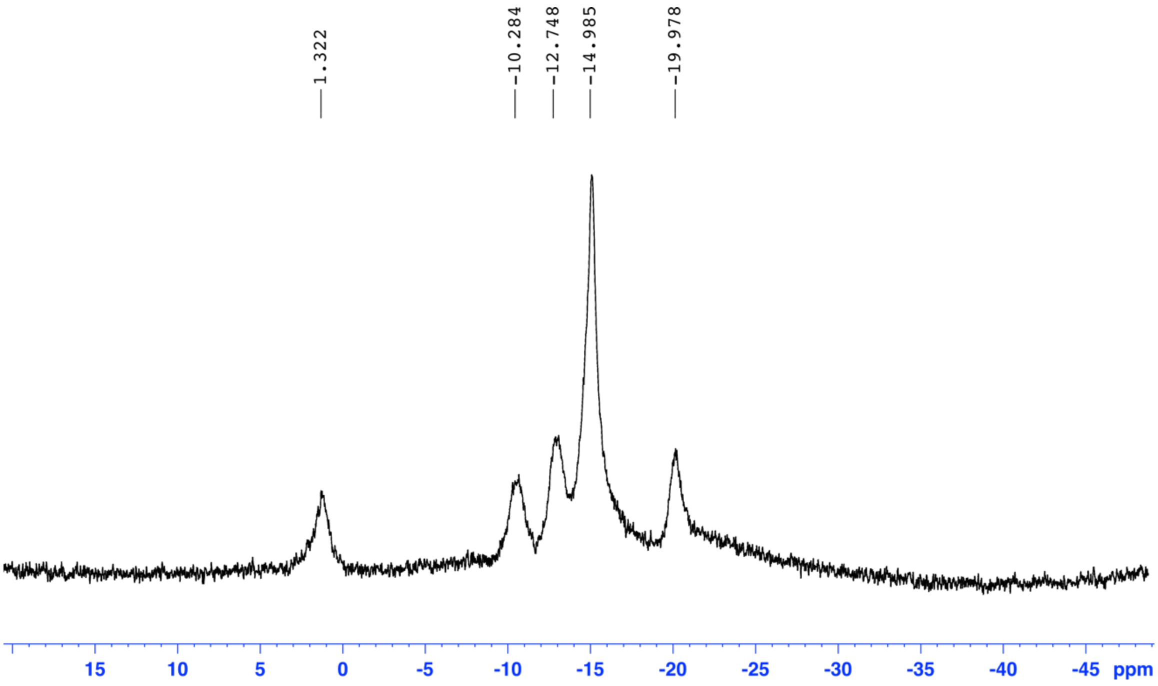

Figure S-33. The $^{11}B\{^1H\}$ NMR spectrum of (POB(I)OP)Ru(I)(CO) (**5**) in C_6D_6.

$^{11}B\{^1H\}$ NMR (C_6D_6): δ 1.3 (*B*Ru), -10.3 (*B*H), -12.8 (*B*H), -15.0 (*B*H and *B*I), -20.0 (*B*H).

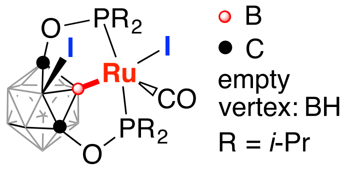

5

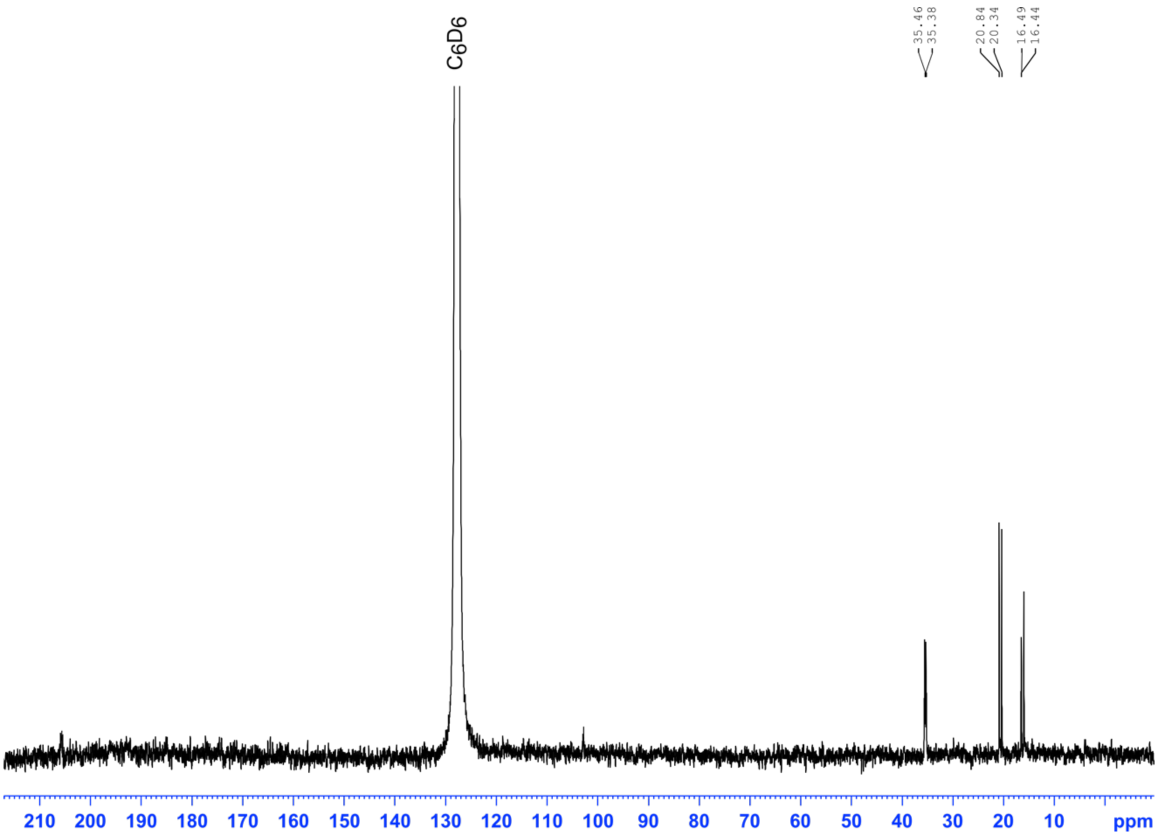

Figure S-34. The ^{13}C NMR spectrum of (POB(I)OP)Ru(I)(CO) (**5**) in C_6D_6.

^{13}C (C_6D_6): δ 206.1 (Ru-*C*O), 102.9 (*C*$_2$B$_{10}$), 35.4 (P(*C*H(CH$_3$)$_2$), 20.5(P(*C*H(CH$_3$)$_2$), 16.4 (P(CH(*C*H$_3$)$_2$).

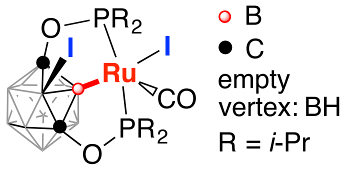

5

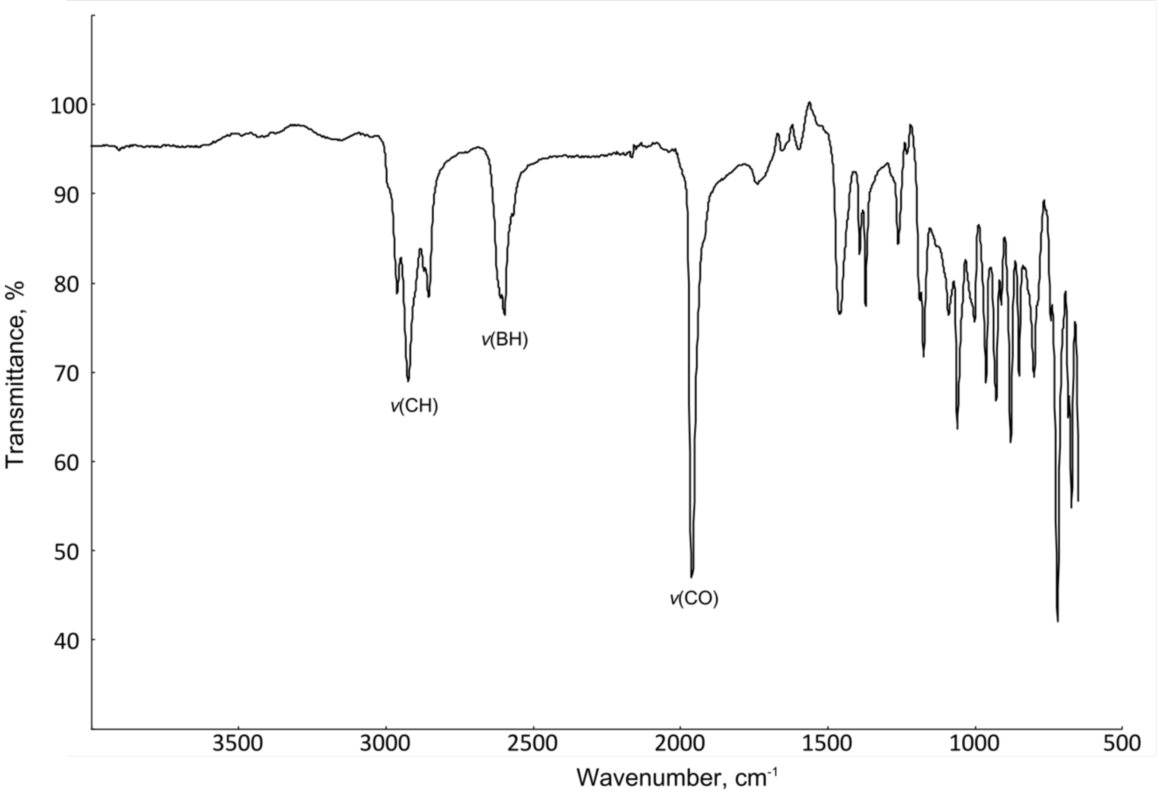

Figure S-35. The ATR-FTIR absorption spectrum of a solid sample of (POB(I)OP)Ru(I)(CO) (**5**).

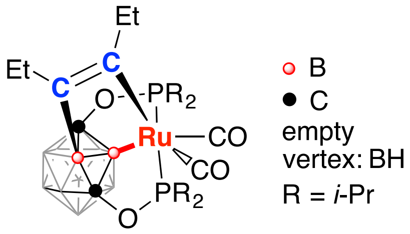

6

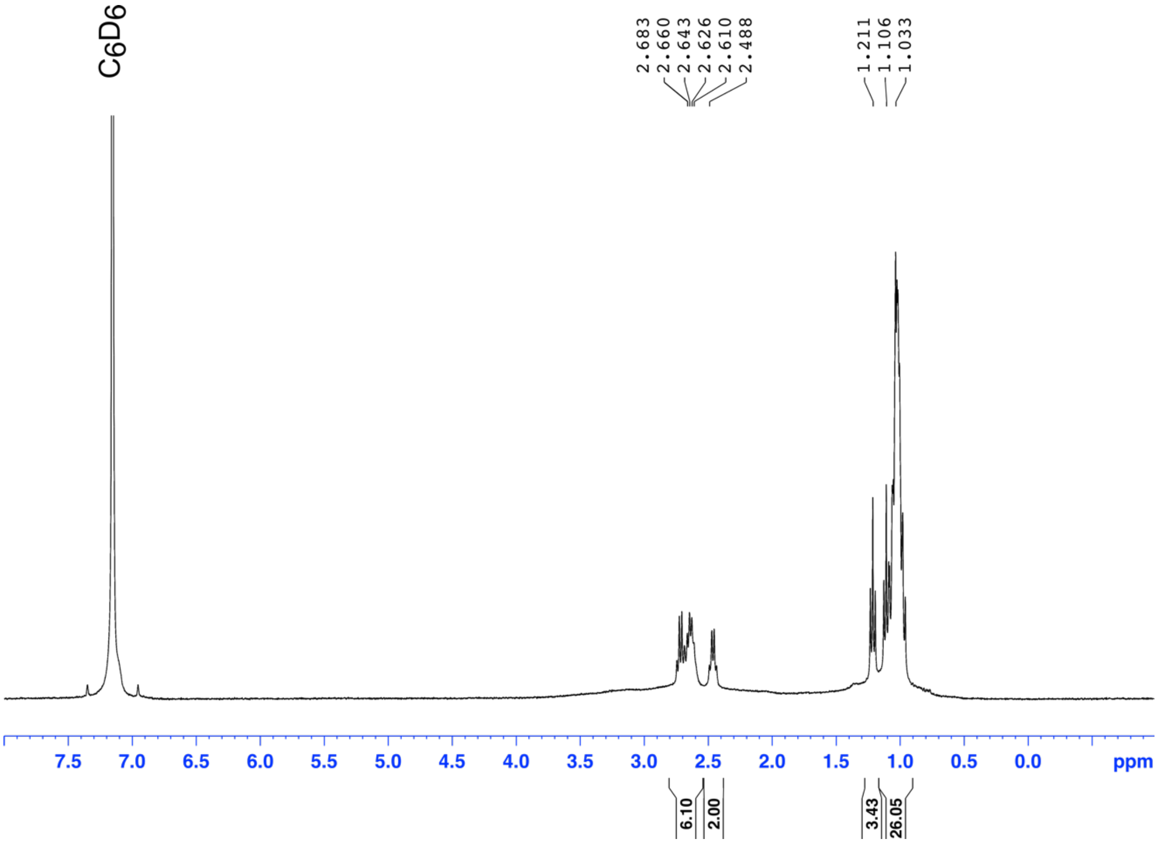

Figure S-36. The ^{1}H NMR spectrum of (POBOP)(EtC=CEt)Ru(CO)$_2$ (**6**) in C_6D_6.

^{1}H NMR (C_6D_6): δ 4.00–1.00 (br, 9H, $C_2B_{10}H_9$), 2.68 – 2.61 (overlapping m, 2H, P(C*H*(CH$_3$)$_2$ and q, 4H, (C)C*H*$_2$CH$_3$), 2.49 (m, 2H, P(C*H*(CH$_3$)$_2$), 1.21 (t, 3H, (C)C*H*$_2$CH$_3$), 1.11–1.03 (overlapping t, 3H, (C)CH$_2$C*H*$_3$ and dd, 24H, P(CH(C*H*$_3$)$_2$).

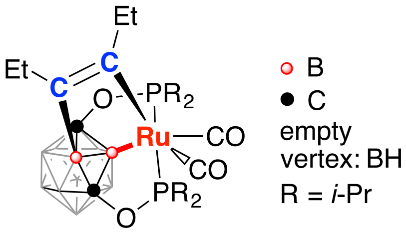

6

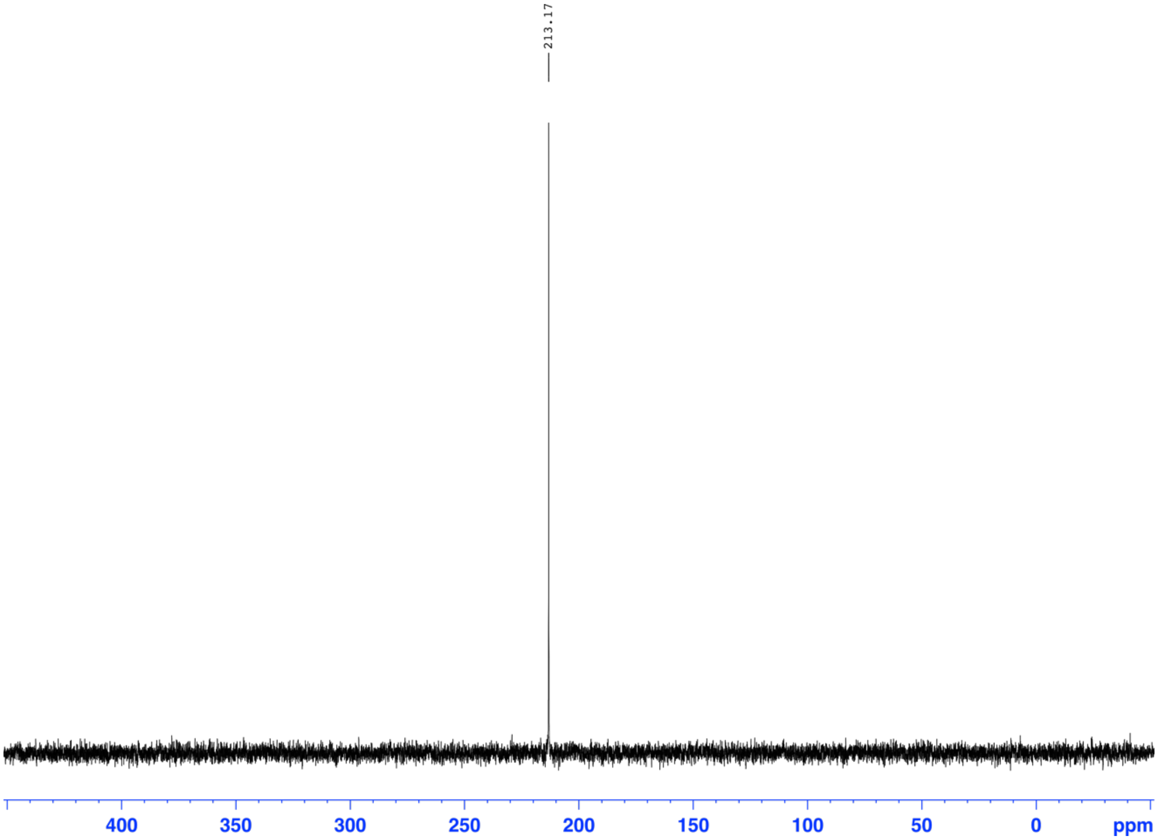

Figure S-37. The ^{31}P NMR spectrum of (POBOP)(EtC=CEt)Ru(CO)$_2$ (**6**) in C_6D_6.

^{31}P NMR (C_6D_6): δ 213.2

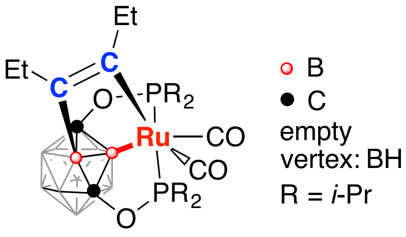

6

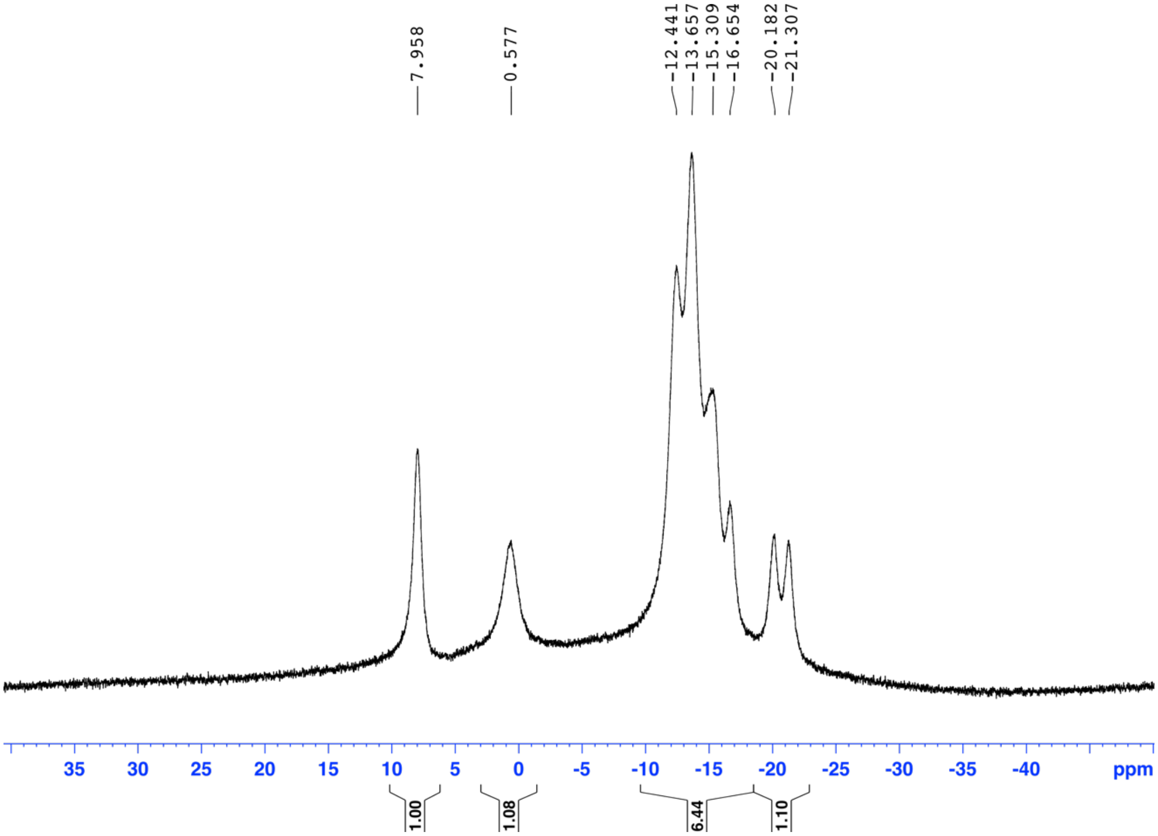

Figure S-38. The ^{11}B NMR spectrum of (POBOP)(EtC=CEt)Ru(CO)$_2$ (**6**) in C_6D_6.

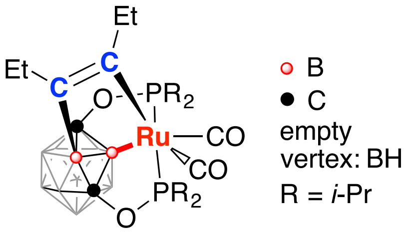

6

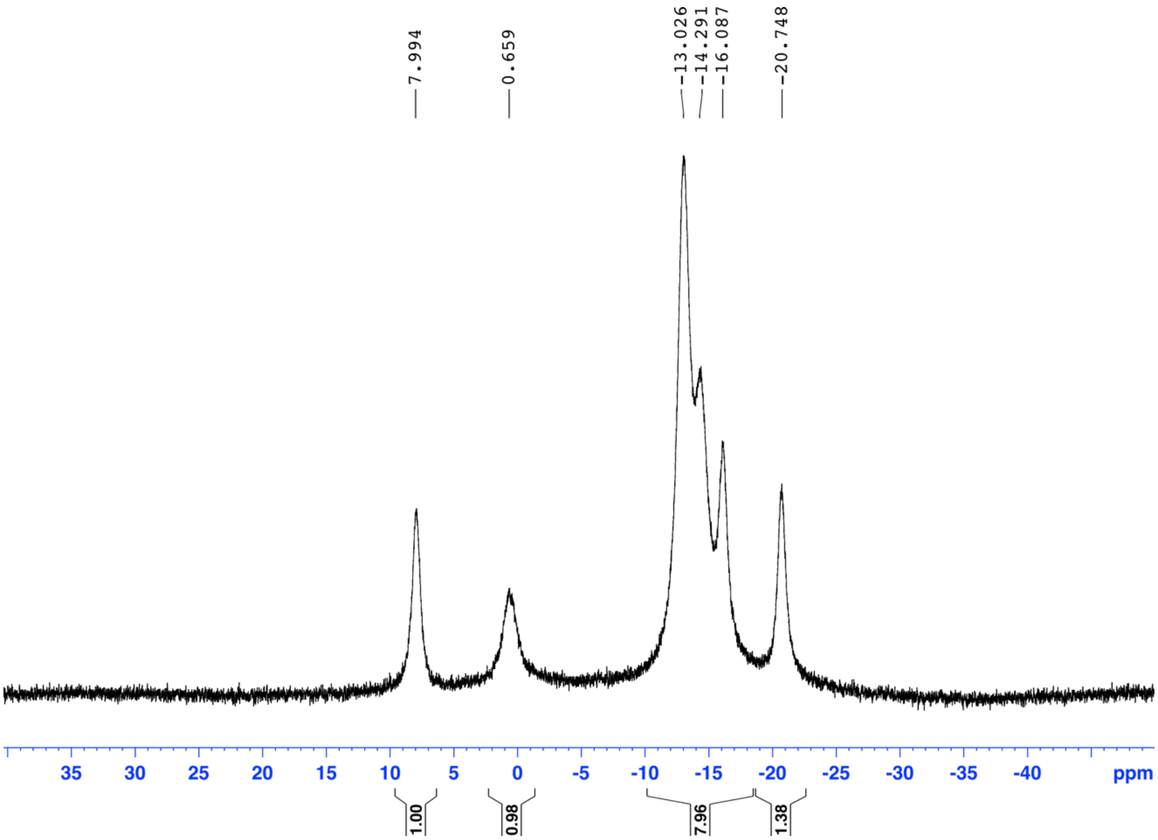

Figure S-39. The $^{11}B\{^{1}H\}$ NMR spectrum of (POBOP)(EtC=CEt)Ru(CO)$_2$ (**6**) in C_6D_6.

$^{11}B\{^{1}H\}$ NMR (C_6D_6): δ 8.0 (*B*Ru), 0.7 (*B*C), -13.0 (*B*H), -14.3 (*B*H), -16.1 (*B*H), -20.8 (*B*H).

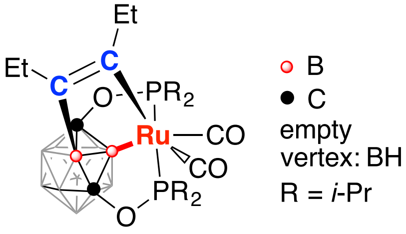

6

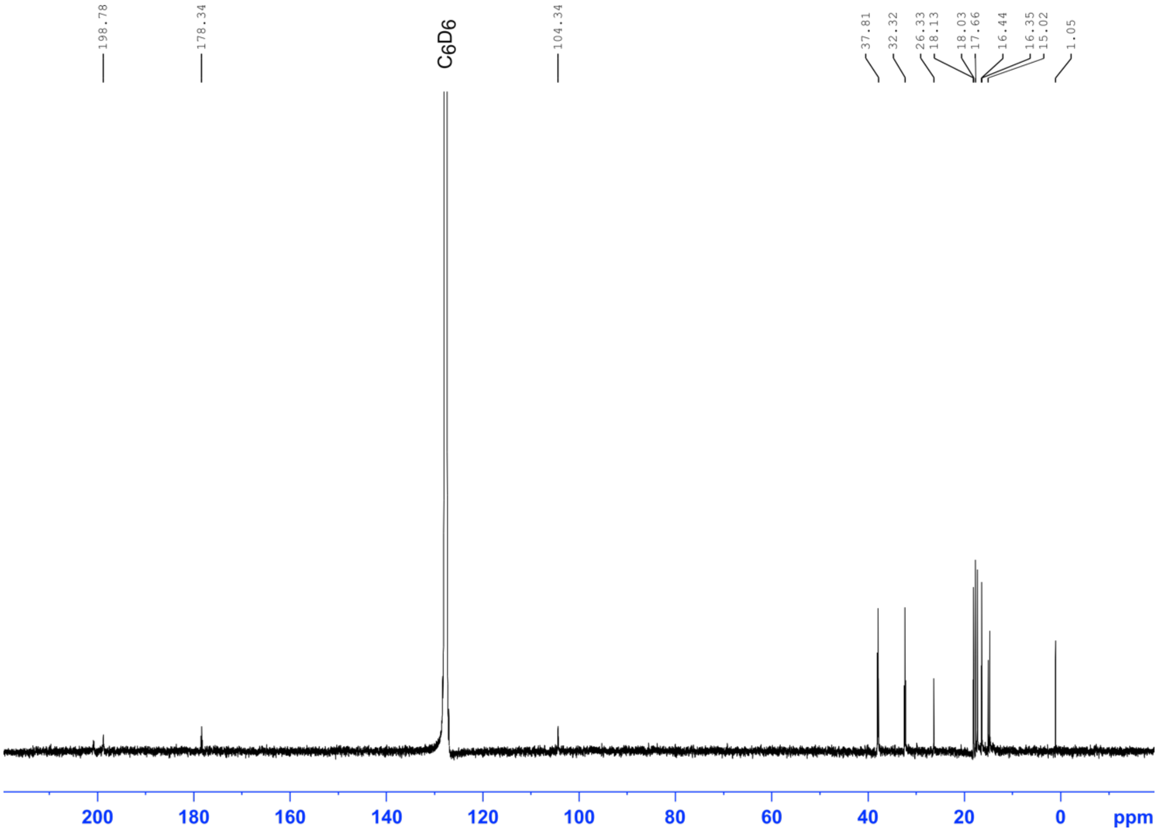

Figure S-40. The ^{13}C NMR spectrum of (POBOP)(EtC=CEt)Ru(CO)$_2$ (**6**) in C_6D_6.

^{13}C NMR (C_6D_6): δ 198.8 (Ru-*C*O), 178.3 (C=*C*CH$_2$CH$_3$), 104.3 (*C*$_2$B$_{10}$), 37.8 (P(*C*H(CH$_3$)$_2$), 32.3 (P(*C*H(CH$_3$)$_2$), 18.1 (P(CH(*C*H$_3$)$_2$), 17.7 (P(CH(*C*H$_3$)$_2$), 16.4 (C=C*C*H$_2$CH$_3$), 16.3 (P(CH(*C*H$_3$)$_2$), 1.05 (C=CCH$_2$*C*H$_3$).

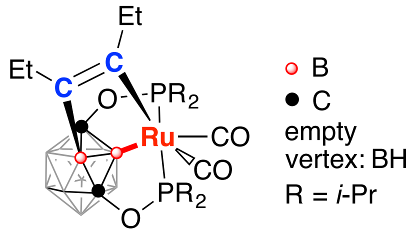

6

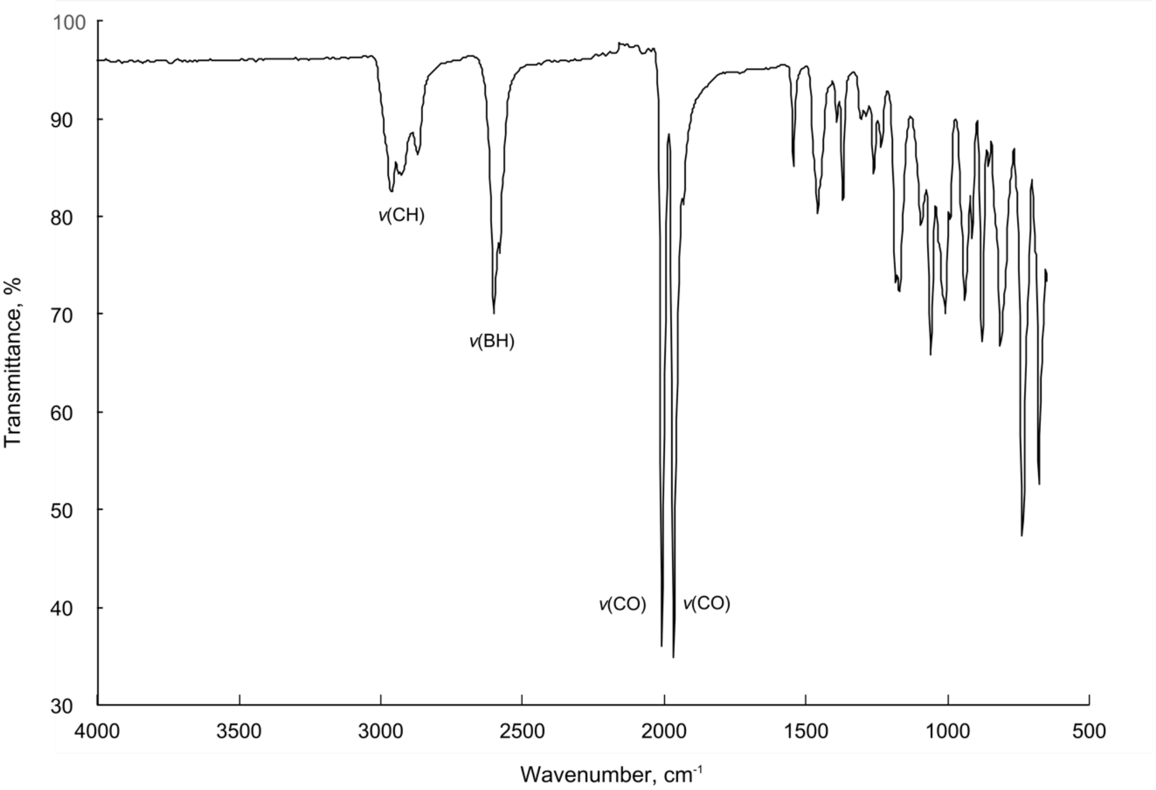

Figure S-41. The ATR-FTIR absorption spectrum of a solid sample of (POBOP)(EtC=CEt)Ru(CO)$_2$ (**6**).

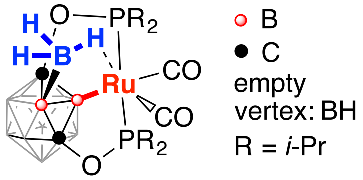

7

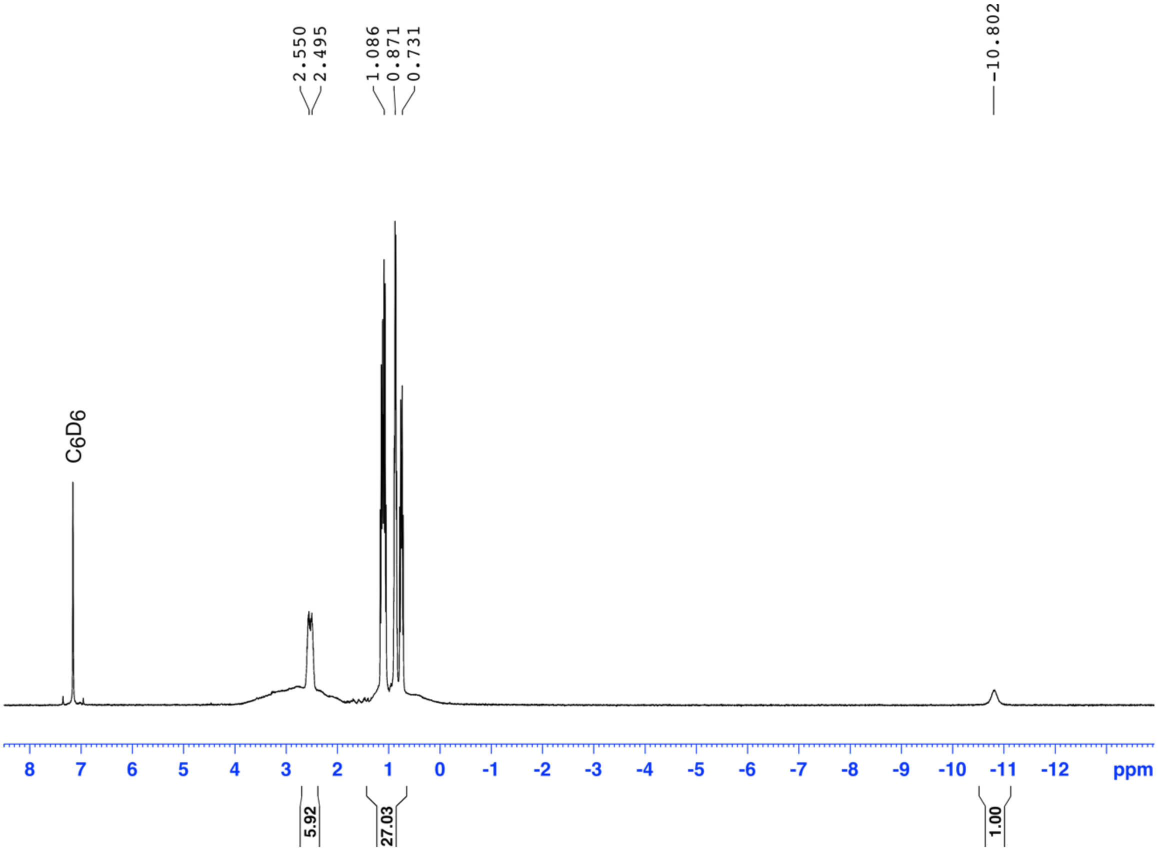

Figure S-42. The ^{1}H NMR spectrum of (POB(BH$_3$)OP)Ru(CO)$_2$ (**7**) in C_6D_6.

^{1}H NMR (C_6D_6): δ 4.00–1.00 (br, 9H, $C_2B_{10}H_9$), 2.50 (overlapping m, 4H, P(C*H*(CH$_3$)$_2$), 1.08 (dd, 12H, P(CH(C*H*$_3$)$_2$)), 0.88 (dd, 6H, P(CH(C*H*$_3$)$_2$)), 0.73 (dd, 6H, P(CH(C*H*$_3$)$_2$)), –10.80 (br, 1H, B–*H*···Ru).

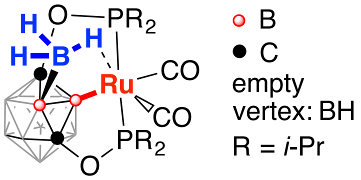

7

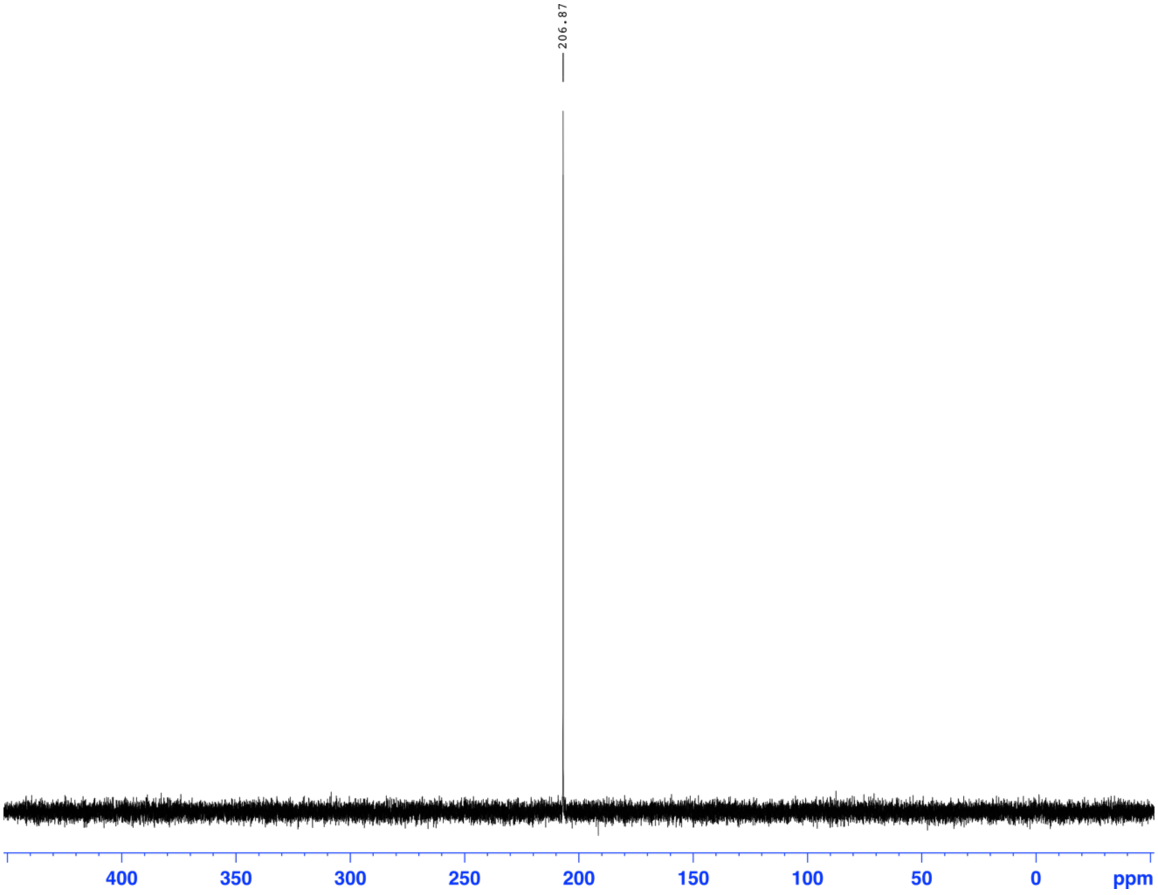

Figure S-43. The ^{31}P NMR spectrum of (POB(BH$_3$)OP)Ru(CO)$_2$ (**7**) in C_6D_6.

^{31}P NMR (C_6D_6): δ 206.9

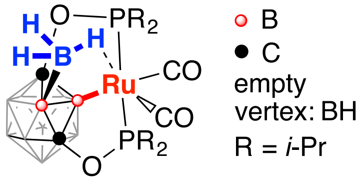

7

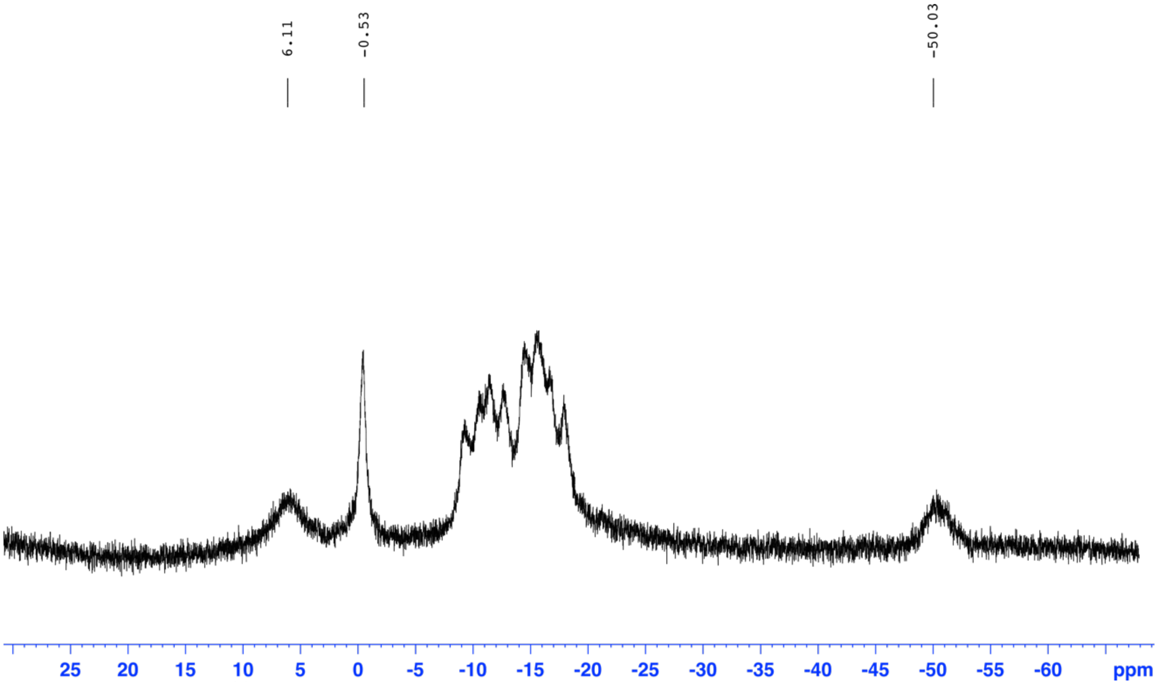

Figure S-44. The ^{11}B NMR spectrum of (POB(BH$_3$)OP)Ru(CO)$_2$ (**7**) in C_6D_6.

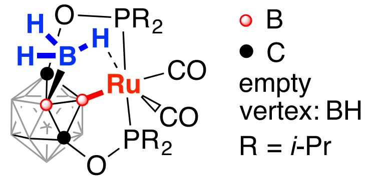

7

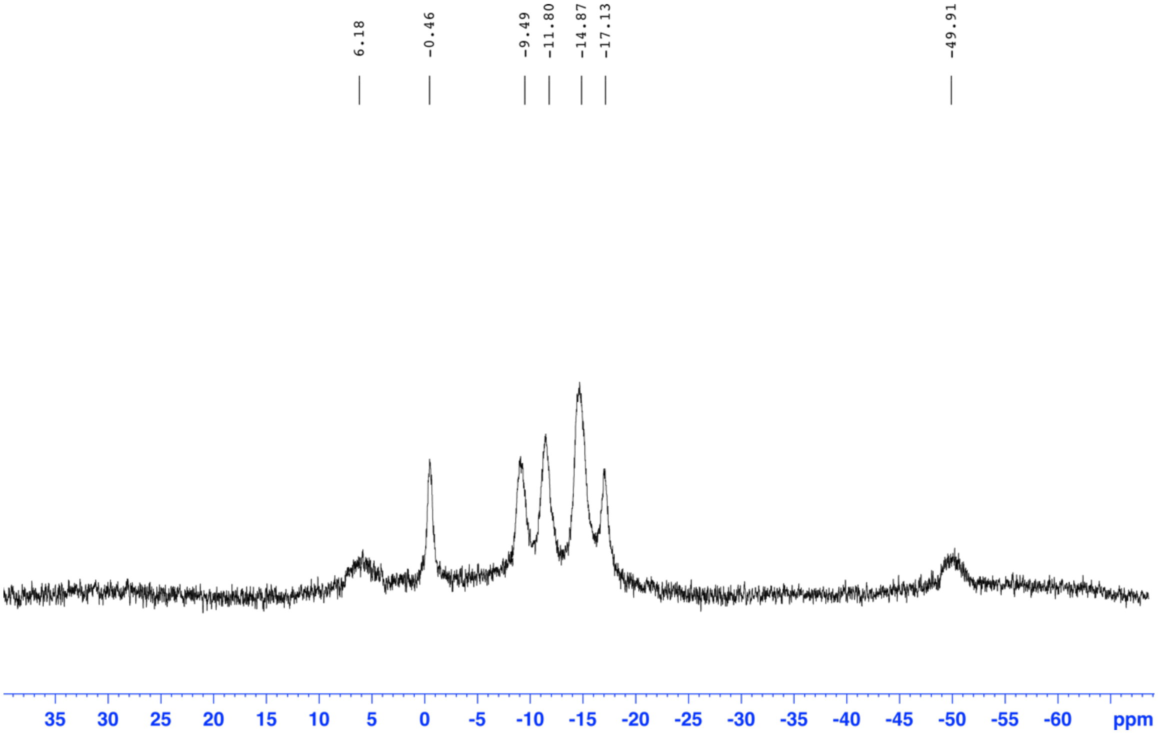

Figure S-45. The $^{11}B\{^1H\}$ NMR spectrum of (POB(BH$_3$)OP)Ru(CO)$_2$ (**7**) in C_6D_6.

$^{11}B\{^1H\}$ NMR (C_6D_6): δ 6.18 (*B*(BH$_3$)), -0.5 (*B*Ru), -9.5 (*B*H), -11.8 (*B*H), -14.9 (*B*H), -17.1 (*B*H), -49.9 (B(*B*H$_3$)).

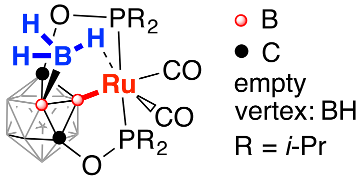

7

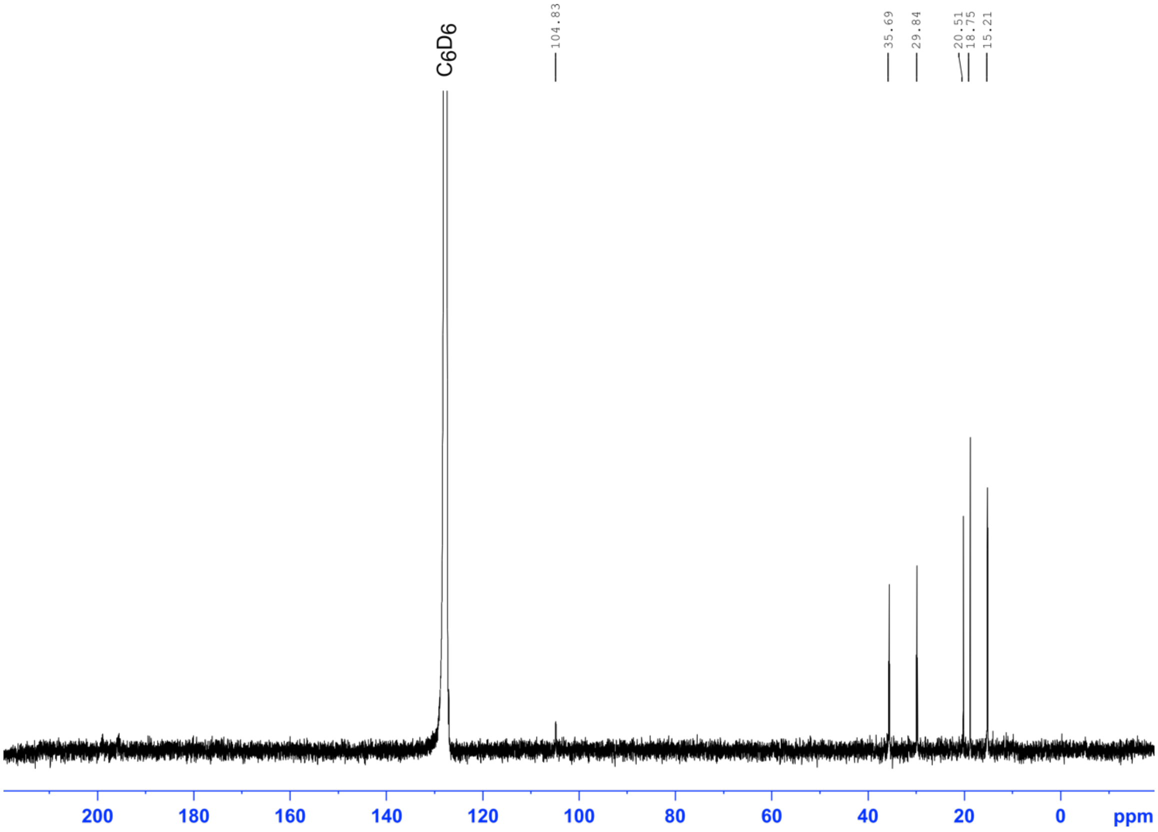

Figure S-46. The ^{13}C NMR spectrum of (POB(BH_3)OP)Ru$(CO)_2$ (**7**) in C_6D_6.

^{13}C NMR (C_6D_6): δ 104.8 (C_2B_{10}), 35.7 (P(*C*H$(CH_3)_2$), 29.8(P(*C*H$(CH_3)_2$), 20.5 (P(CH($C$$H_3$)$_2$), 18.8 (P(CH($C$$H_3$)$_2$), 15.2 (P(CH($C$$H_3$)$_2$).

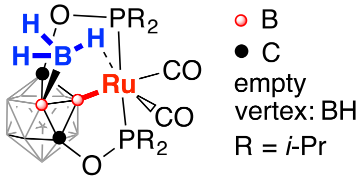

7

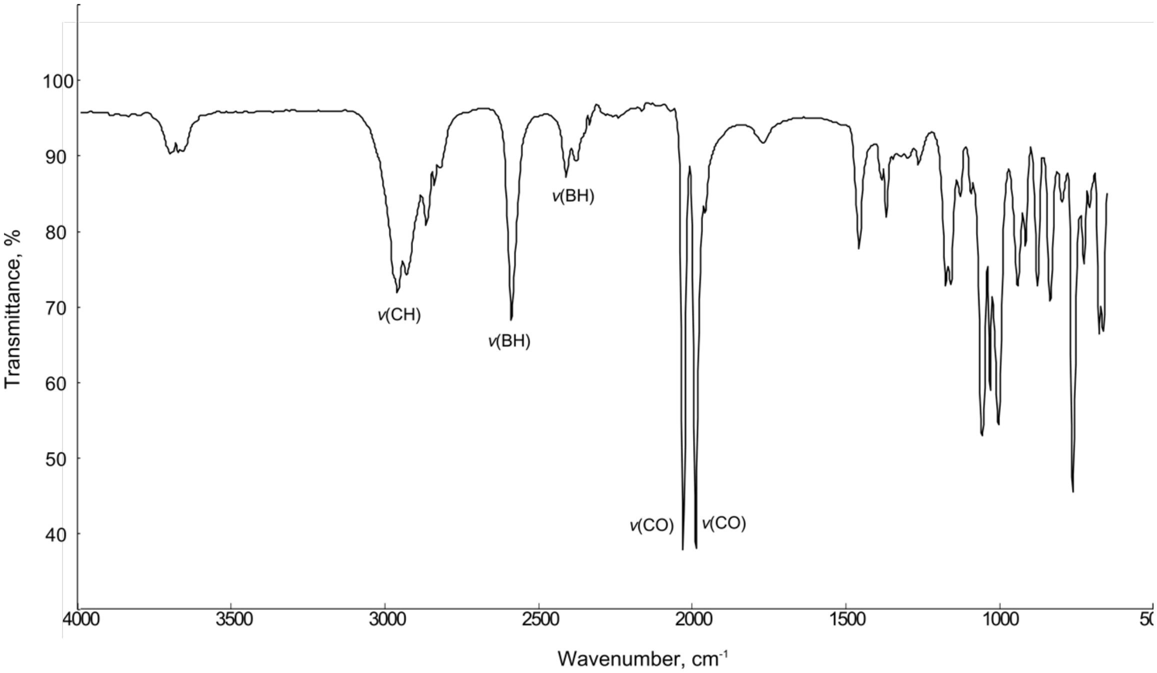

Figure S-47. The ATR-FTIR absorption spectrum of a solid sample of (POB(BH$_3$)OP)Ru(CO)$_2$ (**7**).

Additional details and analysis of computational results.

In the BB-carboryne complex (POBBOP)Ru(CO)$_2$ (**2**), QTAIM atomic charges are +0.34 at Ru, −0.23 at each CO, −0.27 at each "arm", and +0.67 at the $B_{10}C_2H_8$ carborane moiety. Ru donates 0.46 e to CO groups, but it is not obvious how the charge "flows" between the other fragments, and we analyzed the charges in more detail. In the $B_{10}C_2H_8$ fragment, all hydrogens bear almost identical charge of −0.58 *e*. Two borons not bonded to carbon have a charge of 0.62, close to the negative of q(H). Borons bonded to only one carbon bear the charge of 0.91-0.92, which means that each boron donates ca 0.34 *e* to carbon (as a result, carbon in $B_{10}C_2Ru$ are strongly negatively charged, at −1.15, despite their bonding to oxygen). If this increment holds for B1 and B2 (bonded to two carbons at once), each should have donate ca 0.7 e to carbons. Indeed, in $B_{10}C_2H_2$, B1 and B2 bear a charge of +1.26 (of that 0.55 is due to B-to-H donation, and 0.71 is B-to-C donation), whereas in hypothetical $B_{10}C_2$ the charges are reduced to +0.58 *e*. In $B_{10}C_2Ru$, atomic charges of B1 and B2 is +0.53 *e*. This value is smaller than that in $B_{10}C_2$, which indicates that Ru partially donates electrons to boron atoms. The same conclusion is deduced from the distribution of the V(Ru,B) basin population between Ru and B discussed above as well as from the Laplacian map.

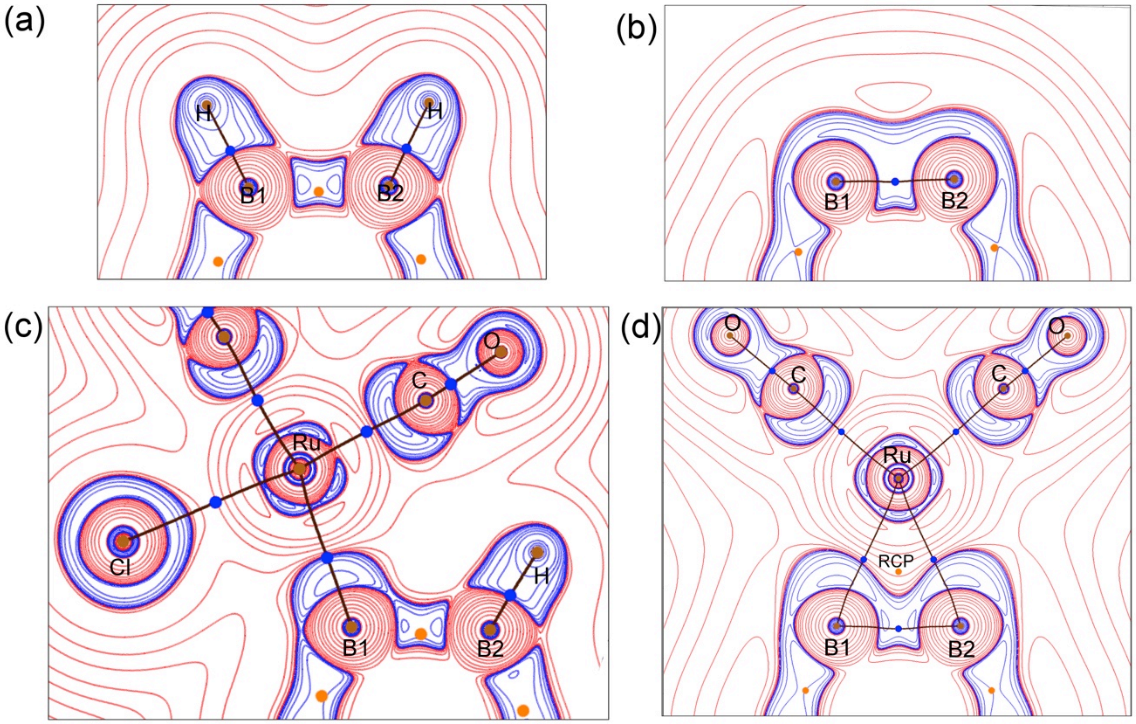

Figure S-49. Laplacian of the electron density (ED) near B1—B2 bond in (a) ligand precursor POBOP-H (**1**), (b) 2,6-dehydro-*m*-carborane, (c) (POBOP)Ru(Cl)$(CO)_2$ (**3**), (d) ruthenium BB-carboryne complex (POBBOP)Ru$(CO)_2$ (**2**). Red lines show negative (depletion of ED) whereas blue lines show positive (concentration of ED). Blue dots are bond critical points. Note the absence of the bond critical point BCP between B1 and B2 in POBOP-H and (POBOP)Ru(Cl)$(CO)_2$.

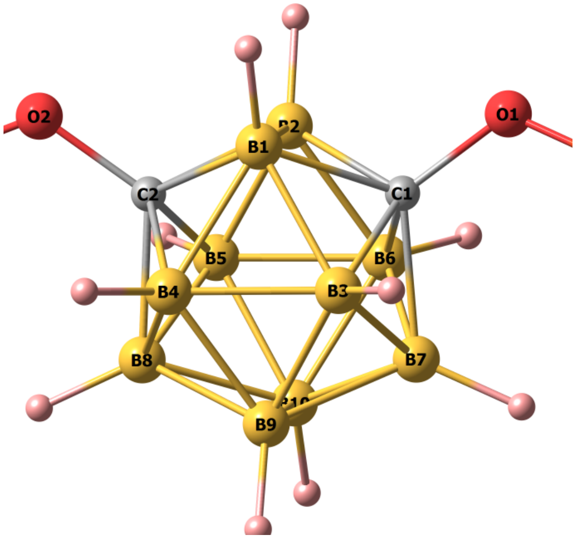

Figure S-50. Numbering scheme for boron atoms used in Table S-35 (hydrogen atoms at B1 and B2 are removed in the hypothetical 2,6-dehydro-*m*-carborane; B1 is coordinated to Ru in (POBOP)Ru(Cl)(CO)$_2$ (**3**); B1 and B2 are coordinated to Ru in (POBBOP)Ru(CO)$_2$ (**2**)).

Table S-51a. Delocalization indices (DI, aka QTAIM bond orders), DFT-optimized interatomic distances (d, Å), and atomic charges for $B_{10}C_2$ moieties and Ru-related fragments.

	POBOP-H (1)			**(POBOP)Ru(Cl)(CO)$_2$ (3)**			**(POBBOP)Ru(CO)$_2$ (2)**			**2,6-dehydro-*m*-carborane**		
	DI	**d**	**Q**	**DI**	**d**	**Q**	**DI**	**d**	**Q**	**DI**	**d**	**Q**
B1-B2	0.11	1.778	1.26/1.26	0.12	1.777	0.70/1.23	0.23	1.709	0.53/0.53	0.79	1.565	0.58/0.58
B1-B3	0.32	1.756	1.26/0.85	0.30	1.773	0.70/0.85	0.33	1.785	0.53/0.91	0.35	1.757	0.58/0.95
B3-B4	0.46	1.754	0.85/0.85	0.49	1.735	0.85/0.85	0.48	1.750	0.91/0.91	0.43	1.772	0.95/0.95
B3-B7	0.32	1.772	0.85/0.82	0.32	1.766	0.85/0.86	0.26	1.799	0.91/0.92	0.26	1.813	0.95/0.91
B3-B9	0.44	1.763	0.85/0.67	0.44	1.756	0.85/0.66	0.44	1.769	0.91/0.62	0.45	1.769	0.95/0.62
B7-B9	0.45	1.763	0.82/0.67	0.45	1.774	0.86/0.66	0.46	1.766	0.92/0.62	0.46	1.765	0.91/0.62
B9-B10	0.41	1.786	0.67/0.67	0.43	1.774	0.66//0.66	0.40	1.798	0.62/0.62	0.40	1.794	0.62/0.62
C1-B1	0.49	1.699	−1.23/1.26	0.52	1.676	−1.15/1.23	0.52	1.720	−1.23/0.53	0.62	1.666	−1.22/0.58
C1-B3	0.50	1.715	−1.23/0.85	0.50	1.704	−1.15/0.85	0.51	1.686	−1.23/0.91	0.49	1.699	−1.22/0.95
C1-B7	0.51	1.706	−1.23/0.82	0.51	1.705	−1.15/0.86	0.53	1.651	−1.23/0.92	0.53	1.665	−1.22/0.91
Ru-B1				0.75	2.131	0.52/0.70	0.69	2.205	0.34/0.53			
Ru-P				0.83	2.351	0.52/1.90	0.89	2.298	0.34/1.95			
Ru-C				1.04	1.950	0.52/1.06	1.22	1.902	0.34/0.99			
C-O				1.38	1.136	1.06/−1.20	1.48	1.145	0.99/−1.22			

Table S-51b. Bond critical parameters[a] for selected pairs of atoms in the ruthenium BB-carboryne complex (POBBOP)Ru(CO)$_2$ (**2**)

	ρ	$\nabla^2\rho$	ε	G/ρ	H/ρ	$\lvert V/G\rvert$	DI
Ru-B1	0.617	1.066	0.360	0.547	-0.426	1.779	0.693
Ru-P	0.713	2.909	0.071	0.719	-0.434	1.603	0.885
Ru-C(O)	1.040	10.571	0.069	1.241	-0.530	1.427	1.215
C-O	3.270	16.191	0.002	2.199	-1.852	1.842	
B1-B2	0.803	-1.437	3.288	0.492	-0.617	2.254	0.234
B1-B3	0.780	-2.306	7.143	0.341	-0.548	2.606	0.326
B3-B4	0.846	-3.510	3.370	0.303	-0.594	2.958	0.475
B3-B7	0.760	-1.918	168.327	0.339	-0.516	2.521	0.263
B3-B9	0.817	-3.010	4.578	0.323	-0.581	2.799	0.442
B7-B9	0.820	-3.245	3.153	0.307	-0.584	2.901	0.463
B9-B10	0.769	-2.304	10.283	0.331	-0.540	2.634	0.395
C-B1	0.855	0.670	0.523	0.963	-0.908	1.943	0.523
C-B3	0.864	1.969	0.509	1.063	-0.903	1.850	0.509
C-B7	0.907	3.475	0.529	1.174	-0.906	1.772	0.529

electronic density ρ [$e\cdot Å^{-3}$] , Laplacian of the density $\nabla^2\rho$ [$e\cdot Å^{-5}$] , elipticity ε, kinetic (G) and total (H) energy densities normalized to ρ [$Ha\cdot e^{-1}$], ratio of the absolute value of the potential energy density to the kinetic energy density ($|V/G|$), delocalization index DI.

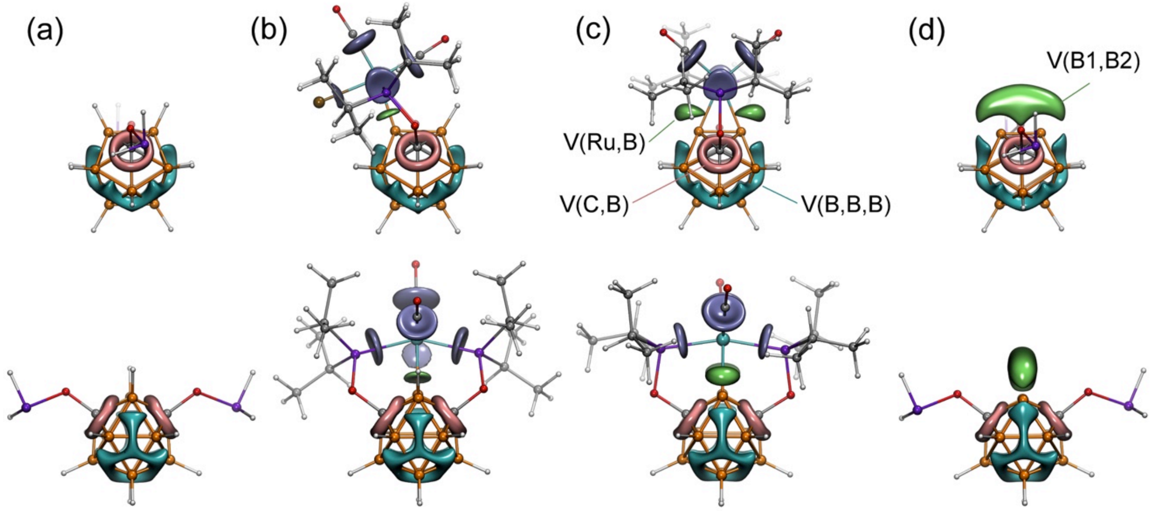

Figure S-52-1. Electron localization function (ELF) isosurfaces (at η = 0.8) for (a) ligand precursor POBOP-H, (b) (POBOP)Ru(Cl)(CO)$_2$ (**3**), (c) ruthenium BB-carboryne complex (POBBOP)Ru(CO)$_2$ (**2**), and (c) hypothetical 2,6-dehydro-*m*-carborane. Trisynaptic V(B,B,B) basins are shown in cyan, disynaptic V(C,B) basins are shown in pink, disynaptic V(Ru,B) or V(B1,B2) basins are shown in light green, and disynaptic V(Ru,C), V(Ru,P), or V(Ru,Cl) basins are shown in violet. All other types of ELF basins are omitted for clarity.

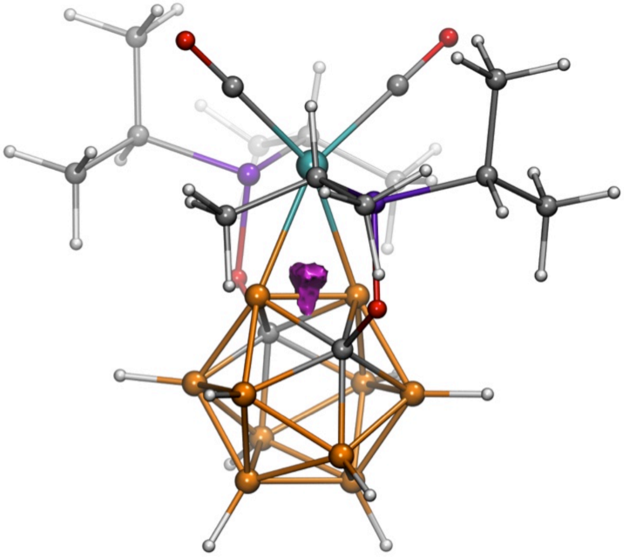

Figure S-52-2. Electron localization function (ELF) isosurface (at η = 0.6) for the three-center V(Ru,B,B) basin in (POBBOP)Ru(CO)$_2$ (**2**). This interaction can be interpreted as weak bonding between Ru and the B–B bond in the (BB)>Ru cycle.

Table S-53. ELF values at the attractor (η), basin populations (Ω_{tot}), and individual atomic contributions ($\Omega_{X,Y,Z}$, where X,Y, and Z denote the atoms participating in a given ELF basin) for selected ELF basins

V(X,Y,Z)	η	Ω_{tot}	Ω_X	Ω_Y	Ω_Z		η	Ω_{tot}	Ω_X	Ω_Y	Ω_Z
(POBBOP)Ru(CO)$_2$						**2,6-dehydro-*meta*-carborane.**					
V(C1,B1)	0.855	1.03	0.83	0.17		V(C1,B1)	0.843	0.89	0.76	0.11	
V(B1,B3,B4)	0.865	1.58	0.73	0.39	0.39	V(B1,B3,B4)	0.866	1.68	0.89	0.35	0.35
V(Ru,B1,B2)	0.672	0.26	0.02	0.12	0.12	V(B1,B2)	0.939	2.38	1.13	1.14	
V(Ru,B1)	0.938	1.69	0.45	1.21							
V(Ru,P1)	0.904	2.25	0.50	1.73							
V(Ru,C3)	0.896	3.06	0.52	2.53							
(POBOP)Ru(Cl)(CO)$_2$						**POBOP-H**					
V(C1,B1)	0.865	1.06	0.91	0.13		V(C1,B1)	0.871	1.10	0.93	0.15	
V(C1,B1,B2)	0.870	1.39	1.03	0.09	0.24	V(C1,B1,B2)	0.877	1.44	1.09	0.08	0.24
V(C2,B1,B2)	0.870	1.39	1.04	0.24	0.09	V(C2,B1,B2)	0.877	1.43	1.09	0.23	0.07
V(B1,B3,B4)	0.865	1.44	0.66	0.36	0.36	V(B1,B3,B4)	0.876	2.50	0.72	0.78	0.82
V(Ru,B1)	0.895	1.73	0.55	1.16							
V(Ru,P1)	0.915	2.17	0.44	1.71							
V(Ru,C3)	0.889	3.14	0.66	2.47							
V(Ru,Cl)	0.840	0.88	0.11	0.77							

X-Ray Structure Determination, (POBBOP)Ru(CO)$_2$ (2)

X-ray intensity data from a colorless flat needle crystal were collected at 100(2) K using a Bruker D8 QUEST diffractometer equipped with a PHOTON 100 CMOS area detector and an Incoatec microfocus source (Mo Kα radiation, λ = 0.71073 Å).[1] The raw area detector data frames were reduced and corrected for absorption effects using the SAINT+ and SADABS programs.[1] Final unit cell parameters were determined by least-squares refinement of 9837 reflections taken from the data set. The structure was solved by direct methods with SHELXT.[2] Subsequent difference Fourier calculations and full-matrix least-squares refinement against F^2 were performed with SHELXL-2014[2] using OLEX2.[3]

The compound crystallizes in the orthorhombic system. The pattern of systematic absences in the intensity data was consistent with the space group *Pna*2$_1$ and *Pnma*, the latter of which was confirmed by structure solution.. The asymmetric unit consists of half of one molecule, which is located on a crystallographic mirror plane. All non-hydrogen atoms were refined with anisotropic displacement parameters. Hydrogen atoms bonded to carbon were located in Fourier difference maps before being placed in geometrically idealized positions included as riding atoms with *d*(C-H) = 1.00 Å and *U*iso(H) = 1.2*U*eq(C) for methine hydrogen atoms and *d*(C-H) = 0.98 Å and *U*iso(H) = 1.5*U*eq(C) for methyl hydrogens. The methyl hydrogens were allowed to rotate as a rigid group to the orientation of maximum observed electron density. Hydrogen atoms bonded to boron were located in Fourier difference maps and refined freely. The largest residual electron density peak in the final difference map is 0.50 e^-/Å^3, located 0.87 Å from C14.

1. APEX2 Version 2014.9-0, SAINT+ Version 8.34A and SADABS Version 2014/4. Bruker Analytical X-ray Systems, Inc., Madison, Wisconsin, USA, 2014.

2. (a) **SHELXT**: Sheldrick, G. M. *Acta Cryst*. **2015**, *A71*, 3-8. (b) **SHELXL:** Sheldrick, G. M. *Acta Cryst.* **2008**, *A64*, 112-122.

3. Dolomanov, O. V.; Bourhis, L. J.; Gildea, R. J.; Howard J. A. K.; Puschmann, H. *J. Appl. Cryst.* **2009**, *42*, 339-341.

Table S-54. Crystal data and structure refinement for (POBBOP)Ru(CO)$_2$ (**2**)

Identification code	BE388
Empirical formula	$C_{16}H_{36}B_{10}O_4P_2Ru$
Formula weight	563.56
Temperature/K	100(2)
Crystal system	orthorhombic
Space group	P*nma*
a/Å	14.5078(6)
b/Å	17.5364(8)
c/Å	10.1577(4)
α/°	90
β/°	90
γ/°	90
Volume/Å^3	2584.27(19)
Z	4
ρ_{calc}g/cm^3	1.448
μ/mm^{-1}	0.753
F(000)	1152.0
Crystal size/mm^3	0.44 × 0.1 × 0.05
Radiation	MoKα (λ = 0.71073)
2Θ range for data collection/°	4.634 to 60.15
Index ranges	$-19 \leq h \leq 20$, $-24 \leq k \leq 24$, $-14 \leq l \leq 13$
Reflections collected	31707
Independent reflections	3872 [R_{int} = 0.0619, R_{sigma} = 0.0442]
Data/restraints/parameters	3872/0/186
Goodness-of-fit on F^2	1.037
Final R indexes [I>=2σ (I)]	R_1 = 0.0300, wR_2 = 0.0576
Final R indexes [all data]	R_1 = 0.0487, wR_2 = 0.0626
Largest diff. peak/hole / e Å^{-3}	0.50/-0.54

X-Ray Structure Determination, (POBOP)Ru(Cl)$(CO)_2$ (3)

X-ray intensity data from a colorless prism were collected at 100(2) K using a Bruker D8 QUEST diffractometer equipped with a PHOTON 100 CMOS area detector and an Incoatec microfocus source (Mo Kα radiation, λ = 0.71073 Å).[1] The raw area detector data frames were reduced and corrected for absorption effects using the SAINT+ and SADABS programs.[1] Final unit cell parameters were determined by least-squares refinement of 9091 reflections taken from the data set. The structure was solved by direct methods with SHELXT.[2] Subsequent difference Fourier calculations and full-matrix least-squares refinement against F^2 were performed with SHELXL-2014[2] using OLEX2.[3]

The compound crystallizes in the orthorhombic system. The pattern of systematic absences in the intensity data was consistent with the space group $P2_12_12_1$, which was verified by structure solution. The asymmetric unit consists of one molecule. All non-hydrogen atoms were refined with anisotropic displacement parameters. Hydrogen atoms bonded to carbon were located in Fourier difference maps before being placed in geometrically idealized positions included as riding atoms with d(C-H) = 1.00 Å and U_{iso}(H) = $1.2U_{\mathrm{eq}}$(C) for methine hydrogen atoms and d(C-H) = 0.98 Å and U_{iso}(H) = $1.5U_{\mathrm{eq}}$(C) for methyl hydrogens. The methyl hydrogens were allowed to rotate as a rigid group to the orientation of maximum observed electron density. Hydrogen atoms bonded to boron were located and refined freely. The largest residual electron density peak in the final difference map is 0.32 $e^-/Å^3$, located 0.96 Å from B3. The absolute structure (Flack) parameter after the final refinement cycle was –0.019(8).

---

1. APEX2 Version 2014.9-0, SAINT+ Version 8.34A and SADABS Version 2014/4. Bruker Analytical X-ray Systems, Inc., Madison, Wisconsin, USA, 2014.

2. (a) **SHELXT**: Sheldrick, G. M. *Acta Cryst.* **2015**, *A71*, 3-8. (b) **SHELXL:** Sheldrick, G. M. *Acta Cryst.* **2008**, *A64*, 112-122.

3. Dolomanov, O. V.; Bourhis, L. J.; Gildea, R. J.; Howard J. A. K.; Puschmann, H. *J. Appl. Cryst.* **2009**, *42*, 339-341.

Table S-57. Crystal data and structure refinement for (POBOP)Ru(Cl)$(CO)_2$ (**3**)

Identification code	BE2190
Empirical formula	$C_{16}H_{37}B_{10}ClO_4P_2Ru$
Formula weight	600.01
Temperature/K	100(2)
Crystal system	orthorhombic
Space group	$P2_12_12_1$
a/Å	11.9543(5)
b/Å	14.3559(6)
c/Å	16.4299(7)
α/°	90
β/°	90
γ/°	90
Volume/Å^3	2819.6(2)
Z	4
ρ_{calc}g/cm^3	1.413
μ/mm^{-1}	0.786
F(000)	1224.0
Crystal size/mm^3	0.28 × 0.24 × 0.18
Radiation	MoKα (λ = 0.71073)
2Θ range for data collection/°	4.434 to 55.146
Index ranges	$-15 \le h \le 15$, $-18 \le k \le 18$, $-21 \le l \le 21$
Reflections collected	102183
Independent reflections	6532 [R_{int} = 0.0828, R_{sigma} = 0.0273]
Data/restraints/parameters	6532/0/352
Goodness-of-fit on F^2	1.026
Final R indexes [I>=2σ (I)]	R_1 = 0.0222, wR_2 = 0.0411
Final R indexes [all data]	R_1 = 0.0279, wR_2 = 0.0425
Largest diff. peak/hole / e Å^{-3}	0.32/-0.35
Flack parameter	-0.019(8)

X-Ray Structure Determination, (POBOP)Ru(C≡CCO$_2$Et)(CO)$_2$ (4)

X-ray intensity data from a colorless plate were collected at 200(2) K using a Bruker D8 QUEST diffractometer equipped with a PHOTON 100 CMOS area detector and an Incoatec microfocus source (Mo Kα radiation, λ = 0.71073 Å).[1] The raw area detector data frames were reduced and corrected for absorption effects using the SAINT+ and SADABS programs.[1] Final unit cell parameters were determined by least-squares refinement of 9996 reflections taken from the data set. The structure was solved by direct methods with SHELXT.[2] Subsequent difference Fourier calculations and full-matrix least-squares refinement against F^2 were performed with SHELXL-2014[2] using OLEX2.[3]

The compound crystallizes in the monoclinic system. The pattern of systematic absences in the intensity data was consistent with the space group $P2_1/c$, which was verified by structure solution. The asymmetric unit consists of one molecule. The C(O)OCH$_2$CH$_3$ part of the -C≡CC(O)OCH$_2$CH$_3$ ligand is disordered and was modeled with three orientations. Total group occupancy was constrained to unity, and the refined fractional population are A/B/C = 0.258(3)/0.429(3)/0.313(3). Like bonds between the disorder components were restrained to be similar in length and displacement parameters for nearly superimposed atoms were held equal. All non-hydrogen atoms were refined with anisotropic displacement parameters except for the disordered methylene and methyl carbons (isotropic). Hydrogen atoms bonded to carbon were placed in geometrically idealized positions included as riding atoms with d(C-H) = 1.00 Å and Uiso(H) = 1.2Ueq(C) for methine hydrogen atoms, d(C-H) = 0.99 Å and Uiso(H) = 1.2Ueq(C) for methylene hydrogens and d(C-H) = 0.98 Å and Uiso(H) = 1.5Ueq(C) for methyl hydrogens. The methyl hydrogens were allowed to rotate as a rigid group to the orientation of maximum observed electron density. Hydrogen atoms bonded to boron were located in difference maps and refined freely. The largest residual electron density peak in the final difference map is 0.56 e$^-$/Å^3, located 0.94 Å from O5A.

1. APEX2 Version 2014.9-0, SAINT+ Version 8.34A and SADABS Version 2014/4. Bruker Analytical X-ray Systems, Inc., Madison, Wisconsin, USA, 2014.

2. (a) **SHELXT**: Sheldrick, G. M. *Acta Cryst.* **2015**, *A71*, 3-8. (b) **SHELXL:** Sheldrick, G. M. *Acta Cryst.* **2008**, *A64*, 112-122.

3. Dolomanov, O. V.; Bourhis, L. J.; Gildea, R. J.; Howard J. A. K.; Puschmann, H. *J. Appl. Cryst.* **2009**, *42*, 339-341.

Table S-59. Crystal data and structure refinement for (POBOP)Ru(C≡CCO$_2$Et)(CO)$_2$ (**4**).

Identification code	BE312a
Empirical formula	$C_{21}H_{42}B_{10}O_6P_2Ru$
Formula weight	661.65
Temperature/K	200(2)
Crystal system	monoclinic
Space group	$P2_1/c$
a/Å	18.6818(8)
b/Å	8.9257(3)
c/Å	19.5607(8)
α/°	90
β/°	91.6060(14)
γ/°	90
Volume/Å^3	3260.4(2)
Z	4
ρ_{calc}g/cm^3	1.348
μ/mm^{-1}	0.612
F(000)	1360.0
Crystal size/mm^3	0.24 × 0.18 × 0.05
Radiation	MoKα (λ = 0.71073)
2Θ range for data collection/°	4.648 to 52.766
Index ranges	$-23 \leq h \leq 23$, $-11 \leq k \leq 9$, $-24 \leq l \leq 24$
Reflections collected	53855
Independent reflections	6658 [R_{int} = 0.0967, R_{sigma} = 0.0524]
Data/restraints/parameters	6658/39/430
Goodness-of-fit on F^2	1.018
Final R indexes [I>=2σ (I)]	R_1 = 0.0389, wR_2 = 0.0722
Final R indexes [all data]	R_1 = 0.0674, wR_2 = 0.0812
Largest diff. peak/hole / e Å^{-3}	0.56/-0.49

X-Ray Structure Determination, (POBOP)Ru(I)(CO) (5)

X-ray intensity data from a yellow parallelogram-shaped plate were collected at 100(2) K using a Bruker D8 QUEST diffractometer equipped with a PHOTON 100 CMOS area detector and an Incoatec microfocus source (Mo Kα radiation, λ = 0.71073 Å).[1] The raw area detector data frames were reduced and corrected for absorption effects using the SAINT+ and SADABS programs.[1] Final unit cell parameters were determined by least-squares refinement of 9434 reflections taken from the data set. The structure was solved by direct methods with SHELXT.[2] Subsequent difference Fourier calculations and full-matrix least-squares refinement against F^2 were performed with SHELXL-2014[2] using OLEX2.[3]

The compound crystallizes in the monoclinic system. The space group *C*2/*m* was identified from the pattern of systematic absences in the intensity data and by successful structure solution. The asymmetric unit consists of half of one $Ru(I)(CO)(C_{14}H_{36}B_{10}IO_2P_2)$ molecule, which is located on a crystallographic mirror plane, and a region of disordered solvent molecules modeled as benzene-d_6. The benzene is disordered about a position of site symmetry 2/*m*, generating four symmetry-equivalent molecules, and thus the occupancy for one independent component was fixed at 0.25. It was refined as a rigid hexagon with *d*(C-C) = 1.39 Å. All non-hydrogen atoms were refined with anisotropic displacement parameters. RIGU and ISOR instructions were applied to the U_{ij} values of the disordered benzene atoms, to prevent physically unrealistic ellipsoids. Hydrogen atoms bonded to non-solvent carbon atoms were located in Fourier difference maps before being placed in geometrically idealized positions and included as riding atoms with *d*(C-H) = 1.00 Å and *U*iso(H) = 1.2*U*eq(C) for methine hydrogen atoms and *d*(C-H) = 0.98 Å and *U*iso(H) = 1.5*U*eq(C) for methyl hydrogens. The methyl hydrogens were allowed to rotate as a rigid group to the orientation of maximum observed electron density. Hydrogen atoms bonded to boron were located in difference maps and refined freely. The C_6D_6 deuterium atoms were placed in geometrically idealized positions included as riding atoms with *d*(C-D) = 0.95 Å and *U*iso(D) = 1.2*U*eq(C) The largest residual electron density peak in the final difference map is 1.79 $e^-/Å^3$, located 0.53 Å from C2S, indicating further disorder than the four-component model used, but a stable disorder model incorporating this peak could not be achieved.

1. APEX2 Version 2014.9-0, SAINT+ Version 8.34A and SADABS Version 2014/4. Bruker Analytical X-ray Systems, Inc., Madison, Wisconsin, USA, 2014.

2. (a) **SHELXT**: Sheldrick, G. M. *Acta Cryst.* **2015**, *A71*, 3-8. (b) **SHELXL:** Sheldrick, G. M. *Acta Cryst.* **2008**, *A64*, 112-122.

3. Dolomanov, O. V.; Bourhis, L. J.; Gildea, R. J.; Howard J. A. K.; Puschmann, H. *J. Appl. Cryst.* **2009**, *42*, 339-341.

Table S-60. Crystal data and structure refinement for (POBOP)Ru(I)(CO) (**5**).

Identification code	BE337_2
Empirical formula	$C_{18}D_3B_{10}H_{36}I_2O_3P_2Ru$
Formula weight	831.42
Temperature/K	100(2)
Crystal system	monoclinic
Space group	C2/m
a/Å	15.7357(8)
b/Å	12.9295(7)
c/Å	15.8165(8)
α/°	90
β/°	103.388(2)
γ/°	90
Volume/Å^3	3130.5(3)
Z	4
ρ_{calc}g/cm^3	1.764
μ/mm^{-1}	2.596
F(000)	1604.0
Crystal size/mm^3	0.24 × 0.1 × 0.04
Radiation	MoKα (λ = 0.71073)
2Θ range for data collection/°	4.556 to 65.266
Index ranges	$-23 \leq h \leq 23$, $-19 \leq k \leq 19$, $-23 \leq l \leq 23$
Reflections collected	95071
Independent reflections	5939 [R_{int} = 0.0301, R_{sigma} = 0.0130]
Data/restraints/parameters	5939/42/228
Goodness-of-fit on F^2	1.040
Final R indexes [I>=2σ (I)]	R_1 = 0.0188, wR_2 = 0.0452
Final R indexes [all data]	R_1 = 0.0241, wR_2 = 0.0472
Largest diff. peak/hole / e Å^{-3}	1.79/-1.63

X-Ray Structure Determination, (POBOP)(EtC=CEt)Ru(CO)$_2$ (6)

X-ray intensity data from a colorless plate crystal were collected at 100(2) K using a Bruker D8 QUEST diffractometer equipped with a PHOTON 100 CMOS area detector and an Incoatec microfocus source (Mo Ka radiation, l = 0.71073 Å).1 The raw area detector data frames were reduced and corrected for absorption effects using the SAINT+ and SADABS programs.1 Final unit cell parameters were determined by least-squares refinement of 9730 reflections taken from the data set. The structure was solved by direct methods with SHELXT.[2] Subsequent difference Fourier calculations and full-matrix least-squares refinement against $F2$ were performed with SHELXL-2014[2] using OLEX2.3

The compound crystallizes in the monoclinic system. The pattern of systematic absences in the intensity data was consistent with the space group $P2_1/c$, which was verified by structure solution. The asymmetric unit consists of one molecule. All non-hydrogen atoms were refined with anisotropic displacement parameters. Hydrogen atoms bonded to carbon were located in Fourier difference maps before being placed in geometrically idealized positions included as riding atoms with d(C-H) = 1.00 Å and Uiso(H) = 1.2Ueq(C) for methine hydrogen atoms, d(C-H) = 0.99 Å and Uiso(H) = 1.2Ueq(C) for methylene hydrogen atoms and d(C-H) = 0.98 Å and Uiso(H) = 1.5Ueq(C) for methyl hydrogens. The methyl hydrogens were allowed to rotate as a rigid group to the orientation of maximum observed electron density. Hydrogen atoms bonded to boron were located in difference maps and refined freely. The largest residual electron density peak in the final difference map is 1.03 e-/Å3, located 1.62 Å from Ru1.

---

1. APEX2 Version 2014.9-0, SAINT+ Version 8.34A and SADABS Version 2014/4. Bruker Analytical X-ray Systems, Inc., Madison, Wisconsin, USA, 2014.

2. (a) **SHELXT**: Sheldrick, G. M. *Acta Cryst*. **2015**, *A71*, 3-8. (b) **SHELXL:** Sheldrick, G. M. *Acta Cryst*. **2008**, *A64*, 112-122.

3. Dolomanov, O. V.; Bourhis, L. J.; Gildea, R. J.; Howard J. A. K.; Puschmann, H. *J. Appl. Cryst.* **2009**, *42*, 339-341.

Table S-62. Crystal data and structure refinement for (POBOP)(EtC=CEt)Ru(CO)$_2$ (**6**).

Identification code	BE345
Empirical formula	$C_{22}H_{46}B_{10}O_4P_2Ru$
Formula weight	645.70
Temperature/K	100(2)
Crystal system	monoclinic
Space group	$P2_1/c$
a/Å	10.9080(6)
b/Å	13.3367(7)
c/Å	21.9824(11)
α/°	90
β/°	99.305(2)
γ/°	90
Volume/Å^3	3155.8(3)
Z	4
ρ_{calc}g/cm^3	1.359
μ/mm^{-1}	0.626
F(000)	1336.0
Crystal size/mm^3	0.2 × 0.14 × 0.04
Radiation	MoKα (λ = 0.71073)
2Θ range for data collection/°	4.84 to 55.356
Index ranges	$-14 \le h \le 14$, $-17 \le k \le 17$, $-28 \le l \le 28$
Reflections collected	92484
Independent reflections	7374 [R_{int} = 0.0685, R_{sigma} = 0.0366]
Data/restraints/parameters	7374/0/394
Goodness-of-fit on F^2	1.069
Final R indexes [I>=2σ (I)]	R_1 = 0.0364, wR_2 = 0.0726
Final R indexes [all data]	R_1 = 0.0536, wR_2 = 0.0775
Largest diff. peak/hole / e Å^{-3}	1.02/-0.65

X-Ray Structure Determination, $(POB(BH_3)OP)Ru(CO)_2$ (7)

X-ray intensity data from a colorless prism were collected at 100(2) K using a Bruker D8 QUEST diffractometer equipped with a PHOTON 100 CMOS area detector and an Incoatec microfocus source (Mo Ka radiation, l = 0.71073 Å).1 The raw area detector data frames were reduced and corrected for absorption effects using the SAINT+ and SADABS programs.1 Final unit cell parameters were determined by least-squares refinement of 9200 reflections taken from the data set. The structure was solved by direct methods with SHELXT.[2] Subsequent difference Fourier calculations and full-matrix least-squares refinement against *F*2 were performed with SHELXL-2014[2] using OLEX2.3

The compound crystallizes in the monoclinic system. The pattern of systematic absences in the intensity data was consistent with the space group $P2_1/n$, which was verified by structure solution. The asymmetric unit consists of one molecule. All non-hydrogen atoms were refined with anisotropic displacement parameters. Hydrogen atoms bonded to carbon were located in Fourier difference maps before being placed in geometrically idealized positions included as riding atoms with *d*(C-H) = 1.00 Å and *U*iso(H) = 1.2*U*eq(C) for methine hydrogen atoms and *d*(C-H) = 0.98 Å and *U*iso(H) = 1.5*U*eq(C) for methyl hydrogens. The methyl hydrogens were allowed to rotate as a rigid group to the orientation of maximum observed electron density. All hydrogen atoms bonded to boron were located in differecne maps and refined freely. The largest residual electron density peak in the final difference map is 0.48 e-/Å3, located 0.83 Å from B11, midway between the B2-B11 bond.

1. APEX2 Version 2014.9-0, SAINT+ Version 8.34A and SADABS Version 2014/4. Bruker Analytical X-ray Systems, Inc., Madison, Wisconsin, USA, 2014.

2. (a) **SHELXT**: Sheldrick, G. M. *Acta Cryst*. **2015**, *A71*, 3-8. (b) **SHELXL:** Sheldrick, G. M. *Acta Cryst*. **2008**, *A64*, 112-122.

3. Dolomanov, O. V.; Bourhis, L. J.; Gildea, R. J.; Howard J. A. K.; Puschmann, H. *J. Appl. Cryst.* **2009**, *42*, 339-341.

Table S-65. Crystal data and structure refinement for $(POB(BH_3)OP)Ru(CO)_2$ (**7**).

Identification code	BE372
Empirical formula	$C_{16}H_{39}B_{11}O_4P_2Ru$
Formula weight	577.39
Temperature/K	100(2)
Crystal system	monoclinic
Space group	$P2_1/n$
a/Å	9.2907(5)
b/Å	14.0608(7)
c/Å	20.6883(12)
α/°	90
β/°	94.379(2)
γ/°	90
Volume/Å^3	2694.7(3)
Z	4
ρ_{calc}g/cm^3	1.423
μ/mm^{-1}	0.723
F(000)	1184.0
Crystal size/mm^3	0.26 × 0.18 × 0.14
Radiation	MoKα (λ = 0.71073)
2Θ range for data collection/°	4.68 to 65.288
Index ranges	$-14 \leq h \leq 14$, $-21 \leq k \leq 21$, $-31 \leq l \leq 31$
Reflections collected	171375
Independent reflections	9848 [R_{int} = 0.0301, R_{sigma} = 0.0119]
Data/restraints/parameters	9848/0/360
Goodness-of-fit on F^2	1.075
Final R indexes [I>=2σ (I)]	R_1 = 0.0161, wR_2 = 0.0405
Final R indexes [all data]	R_1 = 0.0198, wR_2 = 0.0415
Largest diff. peak/hole / e Å^{-3}	0.48/-0.64

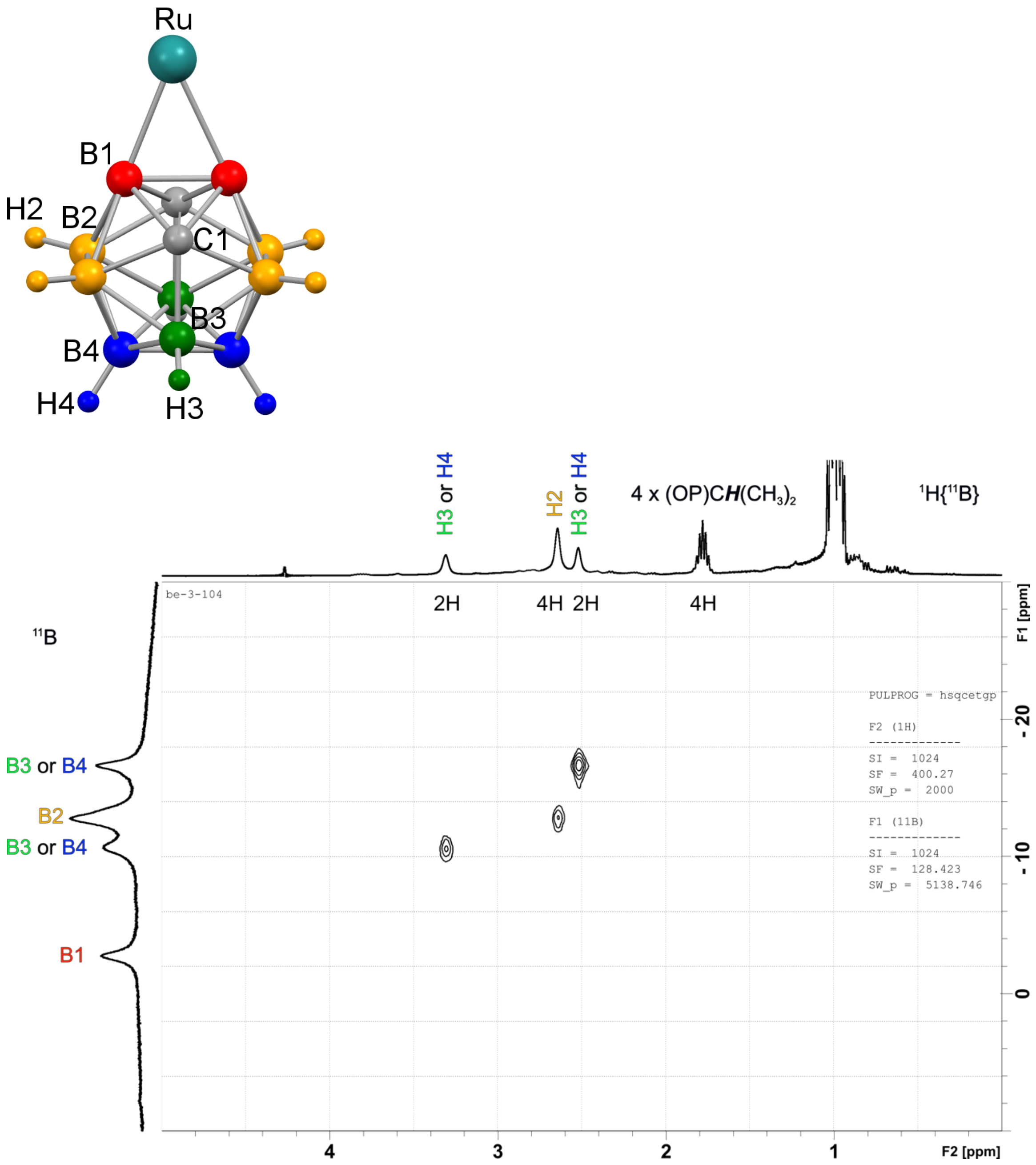

Figure S-66. The ^{1}H-^{11}B HSQC NMR spectrum of the BB-carboryne complex **2** in C_6D_6. The inequivalent types of boron and hydrogen atoms of the cage in **2** are color-coded in red, orange, green, and blue. Note that there are two boron atoms of the (B1) type, four boron atoms/hydrogen atoms of the (B2)/(H2) types, two boron atoms/hydrogen atoms of the (B3)/(H3) types, and two boron atoms/hydrogen atoms of the (B4)/(H4) types.

The expanded chemical shift window for the ^{1}H NMR spectrum (from +7 ppm to –9 ppm) is shown in the Figure S-67 (next page).

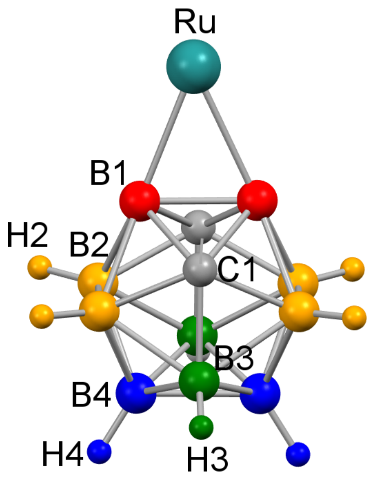

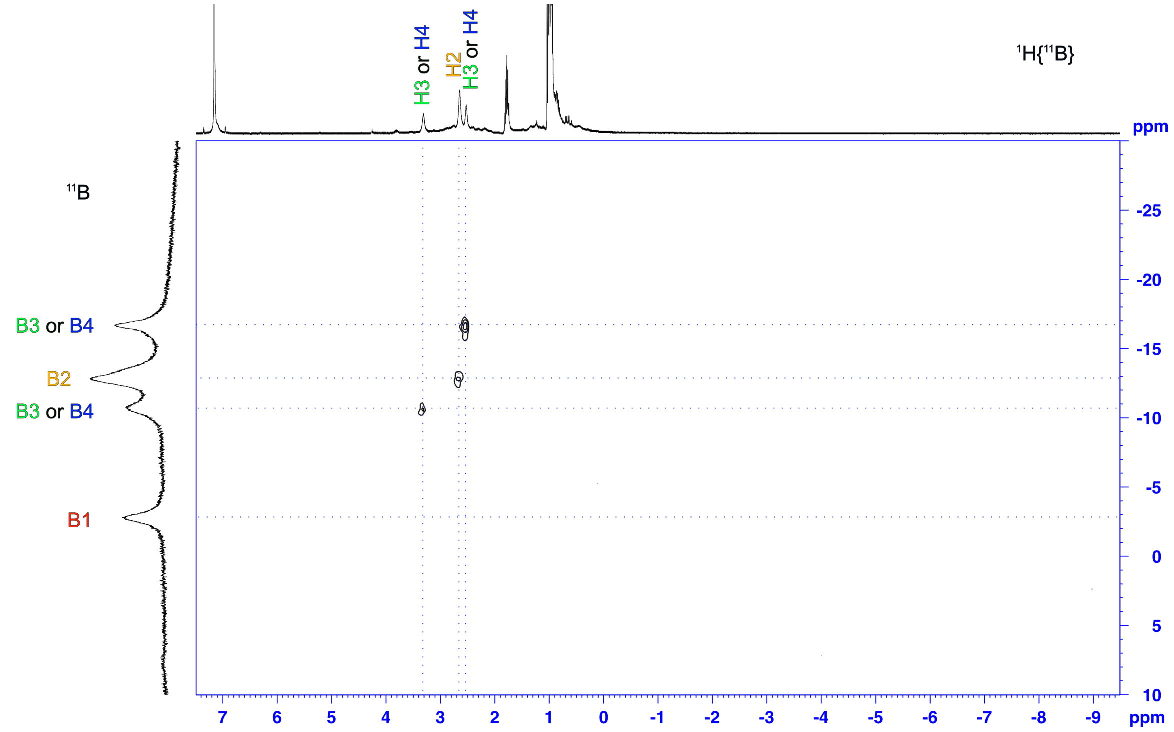

Figure S-67. The ^{1}H-^{11}B HSQC NMR spectrum of the BB-carboryne complex **2** in C_6D_6 (the expanded chemical shift window for the ^{1}H NMR spectrum). The inequivalent types of boron and hydrogen atoms of the cage in **2** are color-coded in red, orange, green, and blue. Note that there are two boron atoms of the (B1) type, four boron atoms/hydrogen atoms of the (B2)/(H2) types, two boron atoms/hydrogen atoms of the (B3)/(H3) types, and two boron atoms/hydrogen atoms of the (B4)/(H4) types.